FINAL TECHNICAL REPORT

SHEAR-WAVE VELOCITIES OF THE POST-PALEOZOIC SEDIMENTS IN THE UPPER MISSISSIPPI EMBAYMENT: COLLABORATIVE RESEARCH BETWEEN THE UNIVERSITY OF KENTUCKY AND THE UNIVERSITY OF MEMPHIS

Award Number: 02HQGR0023

Principal Investigator: Ron L. Street

Kentucky Geological Survey
228 Mining and Mineral Resources Building
Lexington, KY 40506-0107
Email: rstreet@kgs.mm.uky.edu
Phone: 859.257.5500

Co-PI: Edward W. Woolery

Department of Geological Sciences/
Kentucky Geological Survey
University of Kentucky
101 Slone Research Building
Lexington, KY 40506-0053
Phone: 859.257.3016
Fax: 859.257.1147
Email: woolery@uky.edu
http://www.uky.edu/KGS/

Program Element: CU/I
Key Words: Engineering Seismology, Strong ground motion, Amplification

Award Number: 02HQGR0023

SHEAR-WAVE VELOCITIES OF THE POST-PALEOZOIC SEDIMENTS IN THE UPPER MISSISSIPPI EMBAYMENT: COLLABORATIVE RESEARCH BETWEEN THE UNIVERSITY OF KENTUCKY AND THE UNIVERSITY OF MEMPHIS

Ron L. Street and Edward W. Woolery, *Kentucky Geological Survey, University of Kentucky, 228 Mining and Mineral Resources Bldg., Lexington, Ky. 40506-0107,*
Tel: 859.257.3016, Fax: 859.257.1147, Email: woolery@uky.edu

ABSTRACT
Realistic determination of site response and modeling of earthquake induced ground motions in the upper Mississippi Embayment can not be accurately achieved without a reliable P- and S-wave velocity model for the embayment soils/sediments. We have demonstrated from 15 selected sites in the upper embayment that a reliable P- and S-wave velocity model can be achieved by combining data from seismic reflection/refraction profiles, existing deep well-logs, in-situ measurements of shallow Vp and Vs, existing geological models, and arrival time differences between the direct S and converted Sp waves from the bottom of the unlithified sedimentary basin. Because there are significant lateral velocity and structural variations in the unlithified sediment within the embayment, a representative 3-D velocity structure for the embayment can only be established via extensive high-resolution measurements of velocity structures in the region. For example, the lack of systematic measurements in previous S-wave models creates an oversimplification such that lateral velocity variations (especially at shallow depth) are undetected. Consequently, more measurements will be needed to fully develop a reliable 3-D velocity model.

In this investigation, the University of Kentucky performed (1) seismic P-wave and SH-wave reflection/refraction soundings, (2) data analysis and correlations with drill hole logs, and (3) modeling of the P-wave seismic reflections to the bedrock, and SH-wave velocities at selected broadband and short-period seismic station sites to a depth of ~400 m. The University of Memphis performed (1) the compilation of arrival time differences between the direct S and S-to-P converted waves from the bottom of the sediments beneath each selected seismic station (e.g. Chen et al., 1996), (2) the inversion of S-wave velocities of the deeper (>400 m) sediments beneath the selected seismic stations. This report discusses the results from the University of Kentucky tasks.

NONTECHNICAL SUMMARY

This study demonstrates that well-constrained seismic p- and s-wave velocity models of the Post-Paleozoic unlithified sediment in the Upper Mississippi Embayment can be derived by integrated geophysical methods. The thickness of the sediments varies from a few meters near the edges of the Embayment, to several hundreds of meters near the center. These sediment deposits are expected to have a profound influence on the ground motions in the area as a result of a damaging earthquake in the New Madrid seismic zone. Knowledge of the sediment shear-wave velocities allows researchers to assess the hazard posed by earthquakes, as well as recommend mitigation strategies.

INTRODUCTION

The Upper Mississippi Embayment, as described by Toro *et al.* (1992), is a large wedge-shaped syncline that dips to the south, and is filled with several tens to several hundreds of meters of unlithified, post-Paleozoic sediments (Fig. 1).Underlying the embayment, and aligned approximately with its axis is the New Madrid seismic zone, which Cramer (2001) estimated is capable of producing large (> M7) earthquakes at mean-recurrence intervals of 498 years. The effects of the unlithified embayment sediments on ground motions from a damaging earthquake are poorly understood because of the lack of instrumental records, and a lack of reliable *S*-wave velocity data for the deeper (> 100 m) sediments. The sediments in the embayment, as well as the subsurface topography of the bedrock could have a significant effect on the earthquake ground motions in the area. *S*-waves propagating upward through thick layers of unlithified sediments are apt to be amplified and induce resonance at selected frequencies. Resonance can also be set up in a sediment-filled basin if the *S*-waves are incident to the edge of the basin, and the width of the basin is comparable to its depth (Frankel, 1994).

P- and *SH*-wave seismic reflection and refraction data have been acquired at 16 sites (Fig. 2). The sites were chosen for a reasonable spatial distribution, nearness to drillholes that penetrated into bedrock, and nearness to seismograph stations from which earthquake travel-time differences between the direct *S*- and top-of-bedrock converted *Sp*-waves are known. In addition, existing drillhole data, *P*- and *SH*-wave seismic reflection/refraction data, and earthquake travel-time differences between the direct *S*- and top-of-bedrock converted *Sp*-waves were used to estimate the *S*-wave velocities of sediments across the study area.

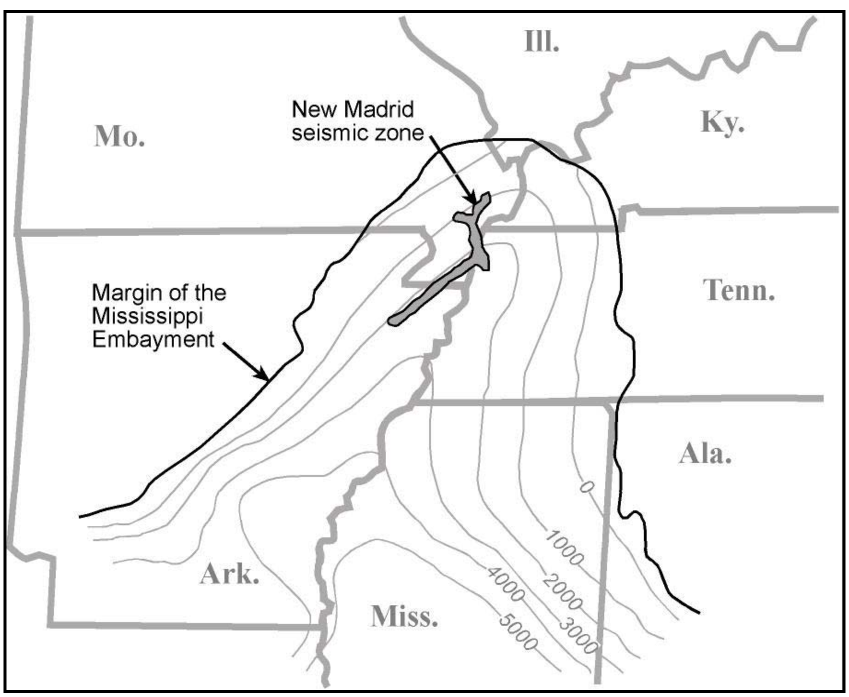

Figure 1. The upper Mississippi embayment has sediment thickness in excess of 600 meters. The contours shown represent feet below mean sea level.

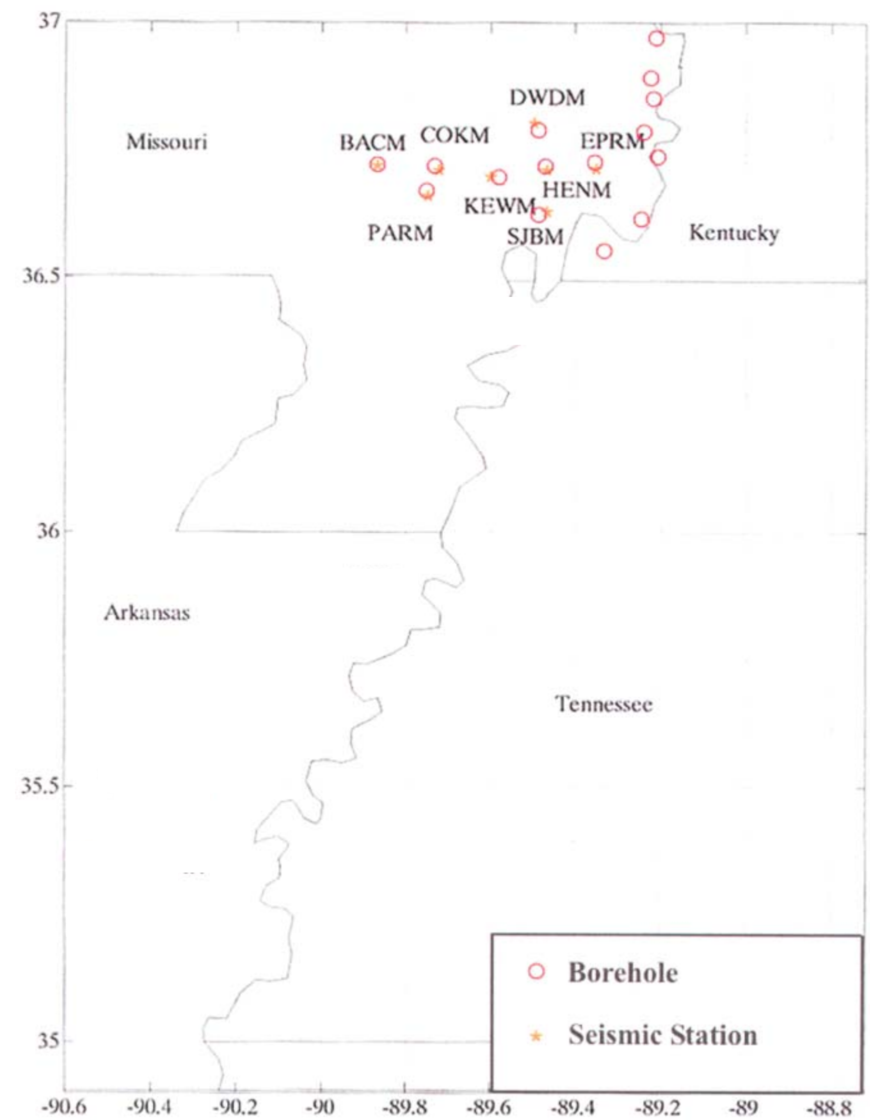

Figure 2. The seismic velocity measurements were conducted at existing borehole sites (red circles) in the upper Mississippi embayment. The gold star indicates location of University of Memphis–CERI seismic stations.

PREVIOUS STUDIES

The early results of a few seismic refraction lines defined a layer of 0.65 km thickness and Vp=1.8 km/sec was introduced to represent the sediments in the Upper Mississippi Embayment (e.g. Mooney et al., 1983; Andrews et al., 1985) where the S-wave velocity of the sedimentary layer was determined under an assumption of Vp/Vs = 3.21 from similar sediments elsewhere. From a 1-D velocity inversion of 3-component PANDA data in the central NMSZ region, Yang (1992) and Chiu et al. (1992) provided the first estimation of an average S-wave velocity of 0.6 km/sec for the sedimentary layer which leads to a Vp/Vs = 3.0.

It has long been recognized from deep wells and from seismic refraction profiles that thickness of the sediments in the Mississippi Embayment region increases toward the south and center of the basin (e.g. Mooney et al., 1983; Andrews et al., 1985; Dart, 1992). From their study of the converted seismic waves occurred from the bottom of the sediments, Chen et al. (1994) and Chen et al. (1996) concluded that the non-vertically incident P- and S-waves from any NMSZ earthquake will not only incident to the surface almost vertically but also will generate large amplitude converted waves across the interface between the overriding sediments and the underlying Paleozoic basement. In their modeling of surface wave dispersion using Vp, Vs and thickness information of the sediments from adjacent well logs, Dorman and Smalley (1994) concluded that the sediments in the embayment serve as an excellent wave-guide to excite very efficient surface waves from earthquakes inside the embayment than that from outside. Based on the relationship between basin resonance and the thickness of basin fill, Bodin and Horton (1999) estimated an average S-wave velocity of 834 m/sec and 960 m thickness for the post-Paleozoic sediments beneath Memphis area. The Post-Paleozoic sediments in the embayment have basically been characterized as a layer or subdivided into many horizontal layers with an average S-wave velocity inside each layer.

Using the previously determined average Vp=1.8 km/sec (e.g. Mooney et al., 1983; Andrews et al., 1985) and thickness of the sediments from nearby deep wells (e.g. Dart 1992), Chen et al. (1996) were able to estimate the variations of average S-wave velocities of the sediments in the ranges from 0.45 to 0.67 km/sec beneath the 40 PANDA stations in the central NMSZ. They concluded that the region of higher S-wave velocity could be correlated to thicker and more compact sediments. Pujol et al. (1997) pointed out that P- and S-wave velocity of the sedimentary section is not a constant from a JHD analysis of earthquake data. Liu et al. (1997) shows significant differences on shallow P- and S-wave velocity profiles of the sediments from in-situ measurements at Shelby Forest, Tennessee; Marked Tree, Arkansas; and Risco, Missouri.

Combining data from well-logs and from some shallow seismic profiles, Mihills (1998) and Mihills and Van Arsdale (1999) were able to subdivide the Post-Paleozoic sediments into layers based on lithology. Gao (1999) and Gao et al. (2001) combined well-log information (Dart, 1992), the geological model of Mihills (1998) and Mihills and Van Arsdale (1999), the in-situ measurement of shallow S-wave velocity information at Marked Tree (Liu et al., 1997), the shallow P- and S-wave velocity information from a few nearby seismic reflection/refraction profiles provided by the University of Kentucky, and the arrival time differences between the direct S and the S-to-P (i.e., *S*- and *Sp*-waves) converted waves to determine first a representative 8-layer P-wave velocity model and then inverted for the deeper S-wave velocities of the sediments.

The results of Gao (1999) and Gao et al. (2001) provided the first reliable estimation of 3-dimensional P- and S-wave velocity model for the embayment sediment; this has improved the hypocentral locations for NMSZ earthquakes. These data have limited shallow P- and S-wave velocity information, and are from a small area in the central NMSZ, however. In addition, lateral variations of the upper most two sedimentary layers were not accounted for in the modeling. This may significantly affect the determination of S-wave velocities for deeper sedimentary layers.

NEHRP CONTRIBUTIONS

The joint research demonstrated that the integration of SH- and P-wave velocity measurements, Δt_{s-s_p} times, drill hole depths, seismic sections, and sonic logs, can provide a well-constrained P- and S-wave velocity model of the post-Paleozoic sediments for ground motion modeling throughout the Upper Mississippi Embayment. Knowledge of the deeper sediments is critical to ground motion modeling (Anderson et al. 1996). In addition, major impedance boundaries within the post-Paleozoic sediments in the Upper Mississippi Embayment will significantly benefit the linearity/nonlinearity study of the ground motions throughout the region.

RESULTS

Well-constrained P-wave and shear-wave velocities of the post-Paleozoic sediments measured at 15sites in the Upper Mississippi Embayment. Since lateral variations of P- and S-wave velocity structure in the embayment are significant (e.g. Liu et al., 1977), the results contribute to the initial establishment of a 3-dimensional Vp and Vs model for realistic 3-D modeling of embayment ground motions. Damage patterns from the 1985 Mexico City, 1988 Armenia, 1989 Loma Prieta, 1994 Northridge, 1999 Chi-Chi and 2002 Hualien, Taiwan earthquakes clearly indicate that basin response, individual site soil conditions, and other geotechnical factors contribute significantly to the nature, severity, and duration of ground shaking. Based on these damage patterns and studies such as those of Bard and Bouchon (1985), Frankel and Vidale (1992), Paolucci et al. (1992), Frankel (1993), and Graves (1993), among others, serious questions have been raised about the validity of ground motion predictions based on 1-D simulations. For example, Frankel (1993) noted that synthetic seismograms obtained from 2- and 3-D modeling of basins exhibited large surface waves produced by the conversion of S-waves at the edge of the basin. Boore (1999) noted that the response spectra of ground motions in the Los Angeles basin might be as much as 5 to 10 times larger than expected from standard response spectra predictions for the basin based on 1-D simulations. We have gradually learned that the geometry of a sedimentary basin as well as velocity characteristics of the sediments will play a significant role on the strong ground motion. We understand roughly the geometry of the sedimentary basin in the Upper Mississippi Embayment from many deep wells. Results from this research provide the initial high-resolution P- and S-wave velocity information for the upper Mississippi embayment region, and is the first step in providing the critical input parameters for realistic assessment of seismic hazard in central U.S.

Table 1 shows the location details of the fifteen seismic sounding sites selected for this study. The seismic soundings acquisition had two primary objectives: 1) produce a 2-dimensional seismic velocity panel approximately coincident with the axis of the Upper Mississippi embayment (i.e., Dorena Line) (Figure 3), and 2) characterize major impedance horizons and integrate geophysical techniques at CERI seismic stations.

Table 1. Seismic Sounding Locations

Dorena Line			
Site	*Latitude*	*Longitude*	*Elevation (m)*
1	36.971	89.207	96
2	36.892	89.222	94
3	36.849	89.209	93
4	36.776	89.244	91
5	36.738	89.215	92
6	36.616	89.241	91
7	36.554	89.332	100
Seismic Stations			
8 (EPRM)	36.724	89.356	90
9 (DWDM)	36.789	89.487	91
10 (HENM)	36.720	89.473	90
11 (SJBM)	36.628	89.489	91
12 (KEWM)	36.696	89.584	88
13 (COKM)	36.715	89.734	87
14 (PARM)	36.671	89.751	87
15 (BACM)	36.723	89.863	88

The seismic soundings acquisition had two primary objectives: 1) produce a 2-dimensional seismic velocity panel approximately coincident with the axis of the Upper Mississippi embayment (i.e., Dorena Line), and 2) characterize major impedance horizons and integrate geophysical techniques at CERI seismic stations. The specific seismic stations are shown in parenthesis in the site column.

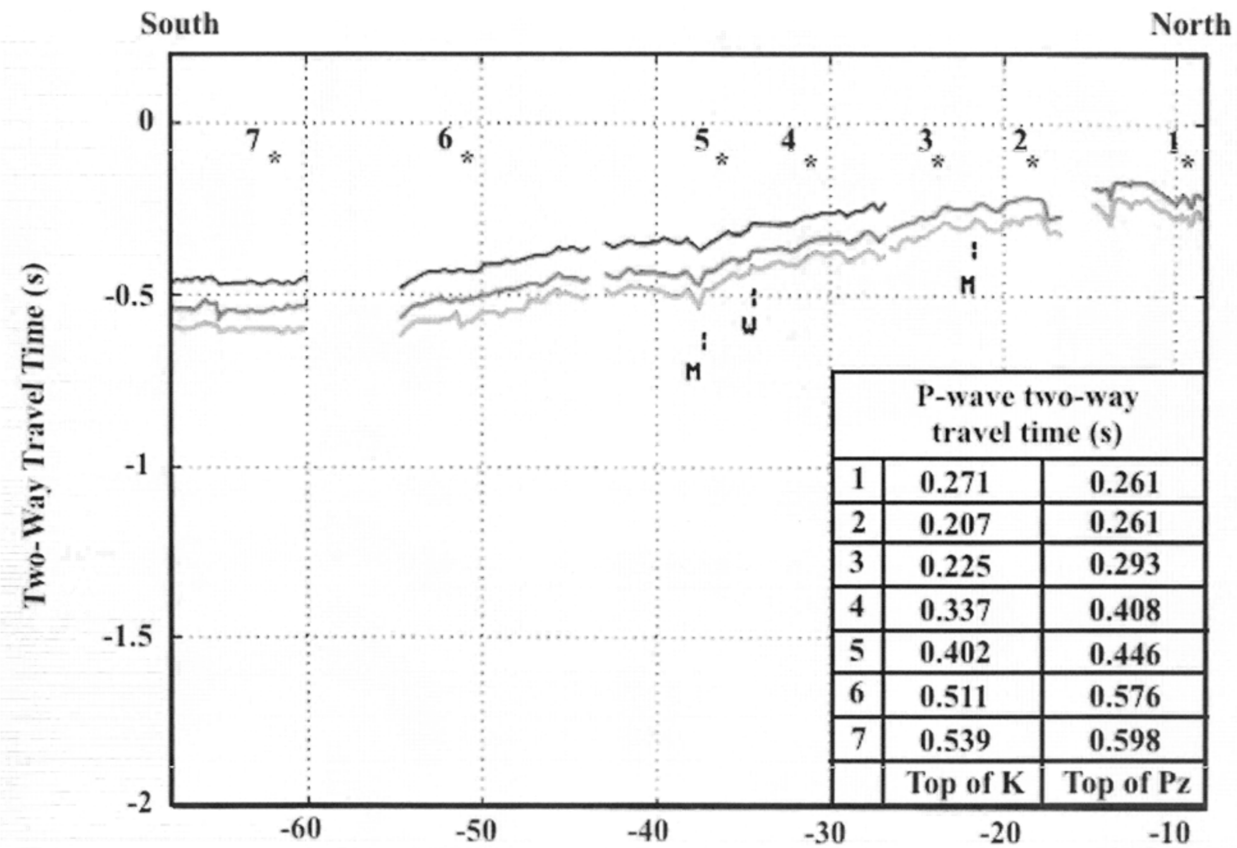

Figure 3. The seismic soundings collected along the Dorena Line in relation to existing industry reflection data. The three horizons represent the interpreted tops of the Paleocene, Cretaceous, and Paleozoic. The inset shows the two-way-travel-time measurements for the tops of the Cretaceous and Paleozoic in our soundings. M (rift margin) and W (Wolf Island fault) are the significant structural features present in the reflection profile.

The *P*-wave data acquisition energy sources were a seismic hammer and vacuum-assisted weight drop. The receivers were inline spreads of twenty-four or forty-eight 40-Hz vertical component geophones spaced at intervals of 6.1 m. The seismic hammer was used at sites where the depth to bedrock was less than 100 m. At some of the sites this included determining the depth to the water table. The weight drop was used at all sites where the depth to bedrock exceeded 100 m. The seismic hammer was used at the 0 offset position, whereas the weight drop was used at stepped-out offsets of one to four times the length of the geophone spread, as well as the zero offset, depending upon the length of the geophone spread, the quality of the recorded signal, and the depth to bedrock. In general, we used 48 geophones spaced at 6.1 m, and stepouts of 0 and 292.6 m with the weight-drop source. The inline-offset panels were combined to form a *P*-wave section representing the range of source-receiver offsets. *SH*-wave data were acquired using a seismic hammer striking an I-beam in the manner described in Street *et al*. (1995). Inline spreads of twenty-four or forty-eight 30-Hz horizontally polarized geophones, spaced at intervals of 6.1 m, were used. The seismic hammer was used at the 0 offset positions at both ends of the geophone spreads. Figure 4 is a representative example of the data quality, as well as, procedure.

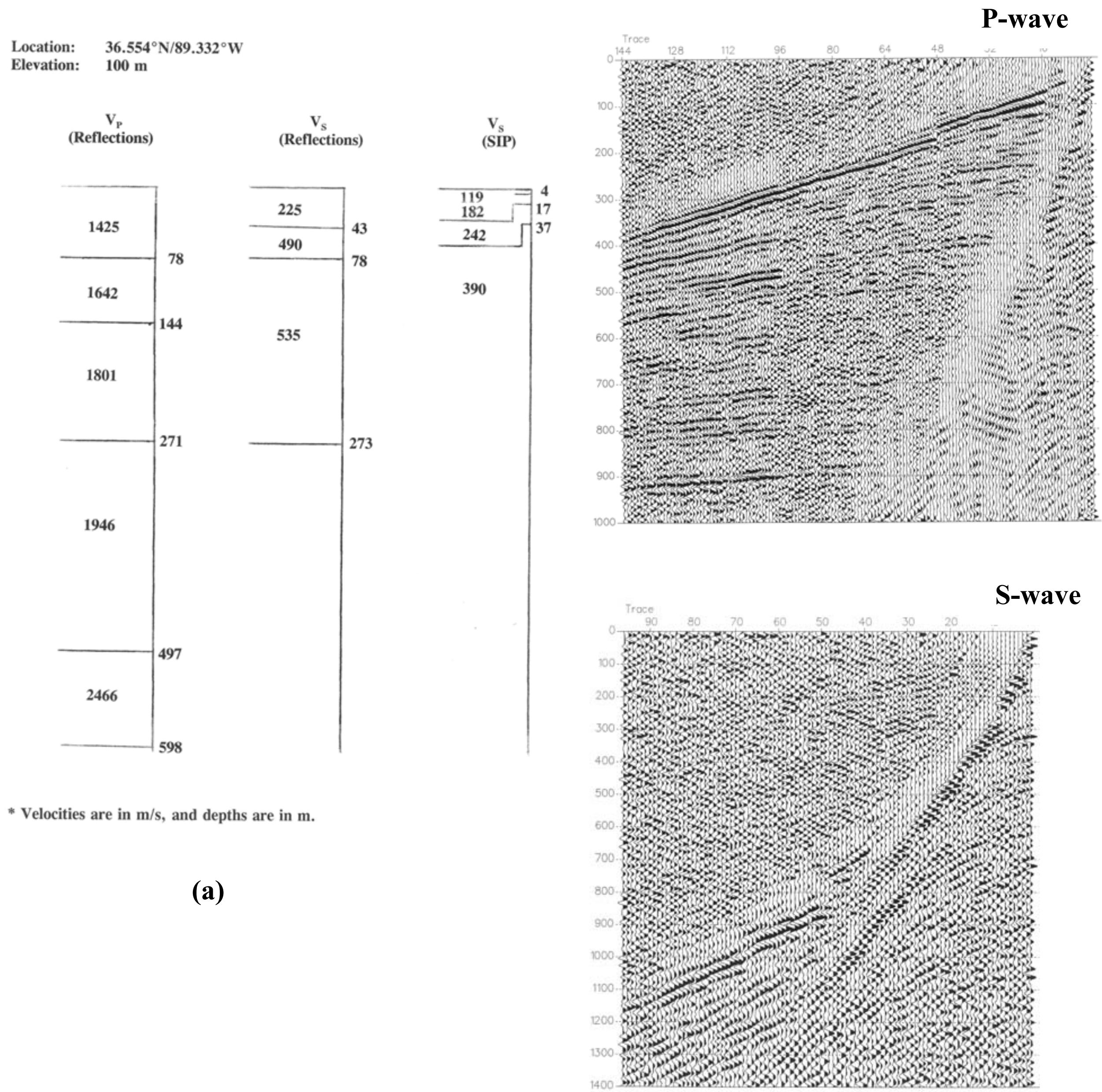

Figure 4. a) P- and S-wave velocity/depth model (depth shown along the side of column; no elevation correction) for the unlithified sediment at the VSAS site. b) The soundings were derived from seismic refraction and reflection walkaway tests.

AVAILABILITY OF DATA

P- and SH-wave seismic reflection and refraction models derived in this study are organized by site, and are given in Appendices A (shallow S-wave velocity profile) and B (site velocity profile). Digital seismic data are archived at the Kentucky Geological Survey as field and processed files. Along with the data files for each site, there is information as to the location of the site, recording parameters, and other pertinent information. The seismic data are stored in standard SEG format, and available upon request. Requests for the information should be directed towards:

Dr. Edward W. Woolery
Department of Geological Sciences
101 Slone Research Building
University of Kentucky
Lexington, KY 40506-0053
Telephone: 859.257.3016
FAX: 859.257.1147
Email: woolery@uky.edu

BIBLIOGRAPHY

Anderson, J.G., Y. Lee, Y. Zeng, and S.Day (1996). Control of strong motion by the upper 30 meters. *Bull. Seism. Soc. Am*. 86, 1749-1759.

Andrews, M.C., W.D. Mooney, and R.P. Meyer (1985). The relocation of microseismity in the northern Mississippi embayment, *J. Geophys. Res*. 90, 10223-10236.

Bard, P.-Y. and M. Bouchon (1985) The seismic response of sediment-filled valleys. Part II. The case of incident P and SV waves. *Bull. Seism. Soc. Am*. 70, 1921-1941.

Benz, H.M., B.A. Chouet, P.B. Dawson, J.C. Lahr, R.A. Page, and J.A. Hole (1996). Three-dimensional P- and S-wave velocity structure of Redoubt Volcano, Alaska, *J. Geophys. Res*. 101(B4), 8111-8128.

Bodin, P. and S. Horton (1999). Broadband microtremor observation of basin resonance in the Mississippi embayment, Central U.S. *Geophys. Res. Letters* 26, 903-906.

Boore, D.M. (1999). Basin waves on a seafloor recording of the 1990 Upland, California, earthquake; Implications for ground motions from a larger earthquake. *Bull. Seism. Soc. Am*. 89, 317-324.

Carver, D. and S.H. Hartzell (1996). Earthquake site response in Santa Cruz, California. *Bull. Seism. Soc. Am*. 86, 55-65.

Chiu, J.M., H. Chen, J. Pujol, S.C. Chiu,M. Withers, (2002), A new earthquake catalog for the New Madrid seismic zone using a preliminary 3-dimensional Vp and Vs model, *Seismo. Res. Lett*. 74(1), 69.

Chen, K.C., J.M. Chiu, and Y.T. Yang (1994). Q_p-Q_s relation in the sedimentary basin of the upper Mississippi embayment using converted phases, *Bull. Seism. Soc. Am*. 84, 1861-1868..

Chen, K.C., J.M. Chiu, and Y.T. Yang (1996). Shear-wave velocity of the sedimentary basin in the Upper Mississippi embayment using *S*-to-*P* converted waves, *Bull. Seism. Soc. Am*. 86, 848-856.

Chen, K.C., (2003). Strong ground motions and damages in Taipei Basin from the Moho reflected seismic waves during the March 31, 2002, Hualien, Taiwan earthquake, submitted March 2003 to Geophy. Res. Lett.

Chiu, J.M., S.C. Chiu, and S.G. Kim, (1997), The significance of the crustal velocity model in local earthquake location from a case example of a PANDA experiment in the central United States, *Bull. Seismo. Soc. Amer*., v. 87, no. 6, 1537-1552.

Chiu, J.M., A.C. Johnston and Y.T. Yang (1992). Imaging the active faults of the central New Madrid seismic zone using PANDA array data. *Seism. Res. Letters,* 63, 375-393.

Dart, R.L. (1992). Catalog of pre-Cretaceous geologic drill-hole data from the Upper Mississippi Embayment: A revision and update of Open-File Report 90-260, *U.S. Geological Open-File Report 92-685*, 253 pp.

Dorman, J., and R. Smalley (1994). Low-frequency seismic surface waves in the Upper Mississippi Embayment, *Seism. Res. Letters,* 65, 137-148.

Frankel, A. (1993). Three-dimensional simulations of ground motions in the San Bernardino Valley, California, for hypothetical earthquakes from a Loma Prieta aftershock. *Bull. Seism. Soc. Am*. 82, 2045-2074.

Frankel, A. and J. Vidale (1992). A three-dimensional simulation of seismic waves in the Santa Clara Valley, California, from a Loma Prieta aftershock. *Bull. Seism. Soc. Am*. 83, 2045-2074.

Gao, F.C. (1999). High-Resolution 3-D Sedimentary Basin and Upper Crustal Structures from 3-D Inversion of PANADA Data, M.S. thesis, The University of Memphis.

Gao, F.C., J.M. Chiu, E. Schweig, J. Pujol, and R. Street (*in preparation*). Determination of V_p and $V_s$profiles in the sedimentary basin of the central New Madrid seismic zone .

Graves, R.W. (1993). Modeling three-dimensional site response effects in the Marina District Basin, San Francisco, California. *Bull. Seism. Soc. Am*. 83, 1242-1263.

Hwang, H., S. Pezeshk, W.W. Lin, J. He, and J.M. Chiu (2001). Generation of synthetic ground motion, Mid-America Center, CD Release 01-02.

Johnston, A.C. (1982). A major earthquake zone on the Mississippi. *Scientific America* 246, 60-68.

Liu, H.P., Y. Hu, J. Dorman, T.S. Chang, and J.M. Chiu (1997). Upper Mississippi Embayment shallow seismic velocities measured in situ, *Engineering Geology,* 46, 313-330.

Mihills, R.K. (1998). A structural anlaysis of the New Madrid seismic zone from contour maps and a three-dimensional model, M.S. Thesis, The University of Memphis.

Mihills, R.K., and R.B. VanArsdale (1999). Late Wisconsin to Holocene New Madrid seismic zone deformation, *Bull. Seism. Soc. Am*. 89, 1019-1024.

Mooney, W.D., M.C. Andrews, A. Ginsberg, D.A. Peters, and R.M. Hamilton (1983). Crustal structure of the northern Mississippi embayment and a comparison with other continental rift zones, *Tectonophysics,* 94, 327-348.

Paolucci, R., M.M. Suarez, and F.J. Sanchez-Sesma (1992). Fast computation of SH seismic response for a class of alluvial valleys. *Bull. Seism. Soc. Am*. 82, 2075-2086.

Pujol, J. A. Johnston, J.M. Chiu, and Y.T. Yang (1997). Refinement of thrust faulting models for the central New Madrid seismic zone, Engineering Geology, 46, 281-298.

Rimrock Geophysics, Inc. (1995). SIPT2 V-4.1 (and other programs), 56 p.

Shen, P. (1999). Simultaneous trave-time inversion for 3-D velocity model and earthquake locations: application to Northridge, California, 1994, mainshock-aftershock sequence, M.S. thesis, The University of Memphis.

Seismic Image Software Ltd. (1996). VISTA 7.0 Notes, 477 pp.

Seht, M.I. and J. Wohlenberg (1999). Microtremor measurements used to map thickness of soft sediments. *Bull Seism. Soc. Am*. 89, 250-259.

Socorro Scientific Software (1998). Refract32, Version 1.8 GS 5.0, 33 pp.

Street, R., E. Woolery, Z. Wang, and J. Harris (1995). A short note on shear-wave velocities and other site conditions at selected strong-motion stations in the New Madrid seismic zone. *Seism. Res. Letters* 66(1), 56-63.

Street, R., E. Woolery, Z. Wang, and I.E. Harik (1997a). Soil classifications for estimating site-dependent response spectra and seismic coefficients for building code provisions in western Kentucky. *Engineering Geology* 46, 331-347.

Street, R., Z. Wang, E. Woolery, J. Hunt, and J. Harris (1997b). Site effects at a vertical accelerometer array near Paducah, Kentucky. *Engineering Geology* 46, 349-367.

Street, R., E. Woolery, Z. Wang, and J. Harris (2001). NEHRP soil classifications for estimating site-dependent seismic coefficients in the central Mississippi River Valley. *Engineering Geology* 62, 123-135.

Wen, K.L., L.Y. Fei, H.Y. Peng, and C.C. Liu, (1995), Site effect analysis from the records of the Wuku downhole array, *TAO,* v. 6, no. 2, 285-298.

Williams, R.A., S. Wood, W.J. Stephenson, J.K. Odum, and R. Street (*accepted*). Surface seismic-refraction/reflection measurements of P- and S-wave velocities, Memphis, Tennessee. *Engineering Geology*.

Woolery, E., R. Street, Z. Wang, and J. Harris (1993). Near-surface deformation in the New Madrid seismic zone as imaged by high resolution SH-wave seismic methods. Seism. Res. Letters 64, 187-200.

Woolery, E., R. Street, Z. Wang, and J. Harris (1996). A P- and SH-wave seismic reflection investigation of the Kentucky Bend Fault Scarp in the New Madrid Seismic Zone. *Seism. Res. Letters* 67, 67-74.

Woolery, E., R. Street, Z. Wang, J. Harris, and J. McIntyre (1999). Neotectonic structures in the central New Madrid seismic zone: evidence from multimode seismic reflection data. *Seism. Res. Letters* 70, 554-576.

Woolery, E. and R. Street (2001). 3D near-surface soil response of earthquake engineering interest from H/V ambient noise ratios. Expanded Abstract, *10th International Conference on Soil Dynamics and Earthquake Engineering,* Philadelphia, Penn., Oct. 7-10.

Woolery, E., and R. Street (2002). Near-surface soils response from H/V ambient noise ratios, *Journal of Soil Dynamics and Earthquake Engineering*, *accepted*.

Yang, Y.T. (1992). Fault zone geometry and crustal velocity structures in the central New Madrid seismic zone using data from the PANADA seismic array, M.S. thesis, The University of Memphis, 72 pp.

APPENDIX A

SHALLOW SHEAR-WAVE REFRACTION MODELS

(Note: no refraction plot at Site 13; not in numerical order)

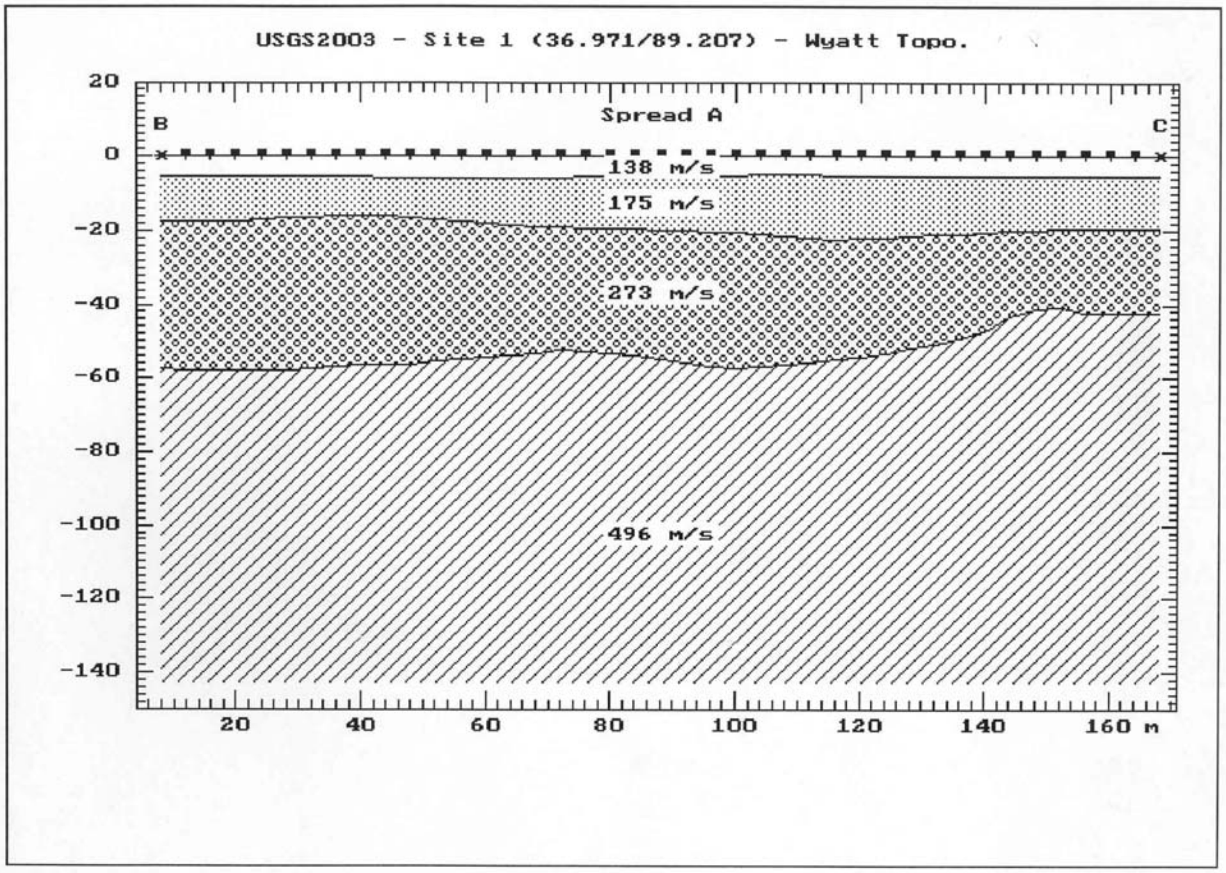

USGS2003 - Site 1 (36.971/89.207) - Wyatt Topo.
Spread A
B
C
138 m/s
175 m/s
273 m/s
496 m/s
20
0
-20
-40
-60
-80
-100
-120
-140
20
40
60
80
100
120
140
160 m

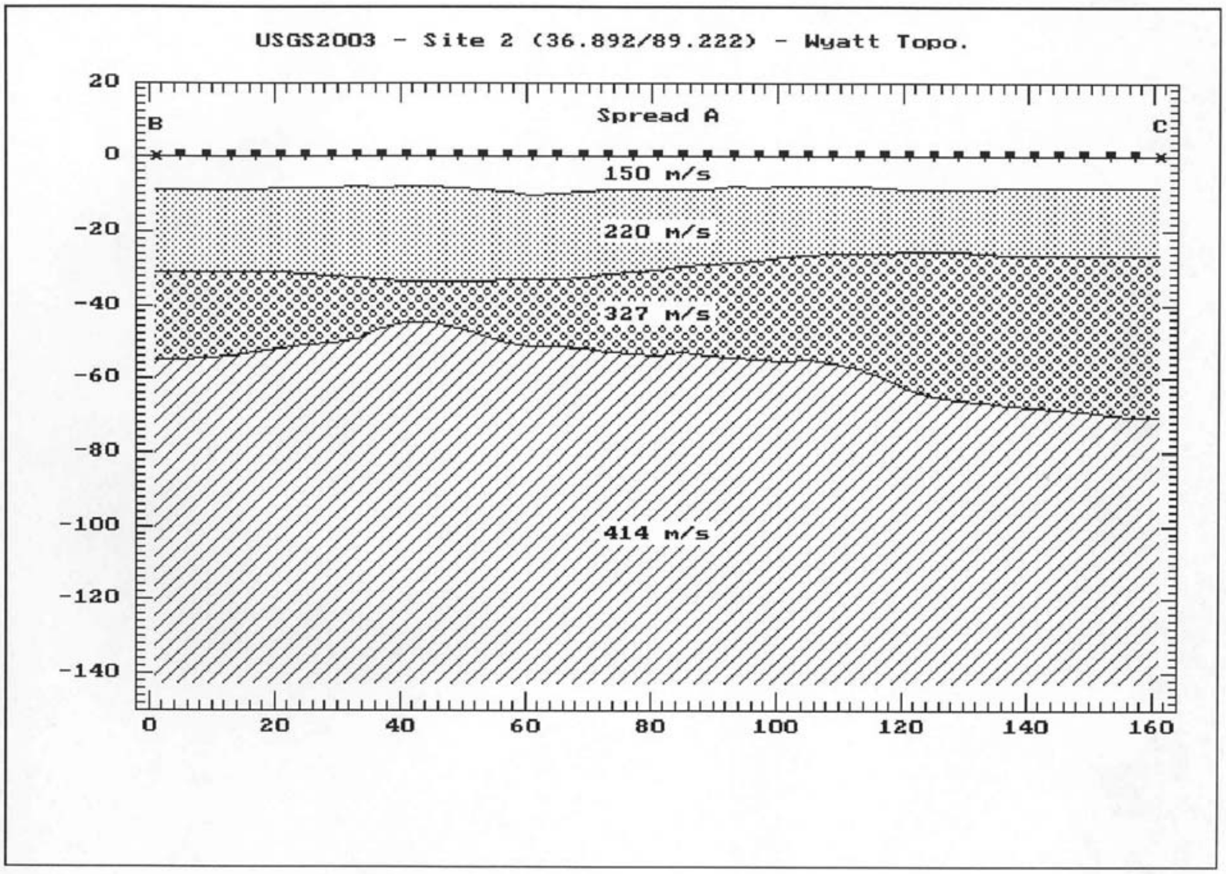
USGS2003 - Site 2 (36.892/89.222) - Wyatt Topo.
Spread A
B
C
150 m/s
220 m/s
327 m/s
414 m/s
20
0
-20
-40
-60
-80
-100
-120
-140
0
20
40
60
80
100
120
140
160

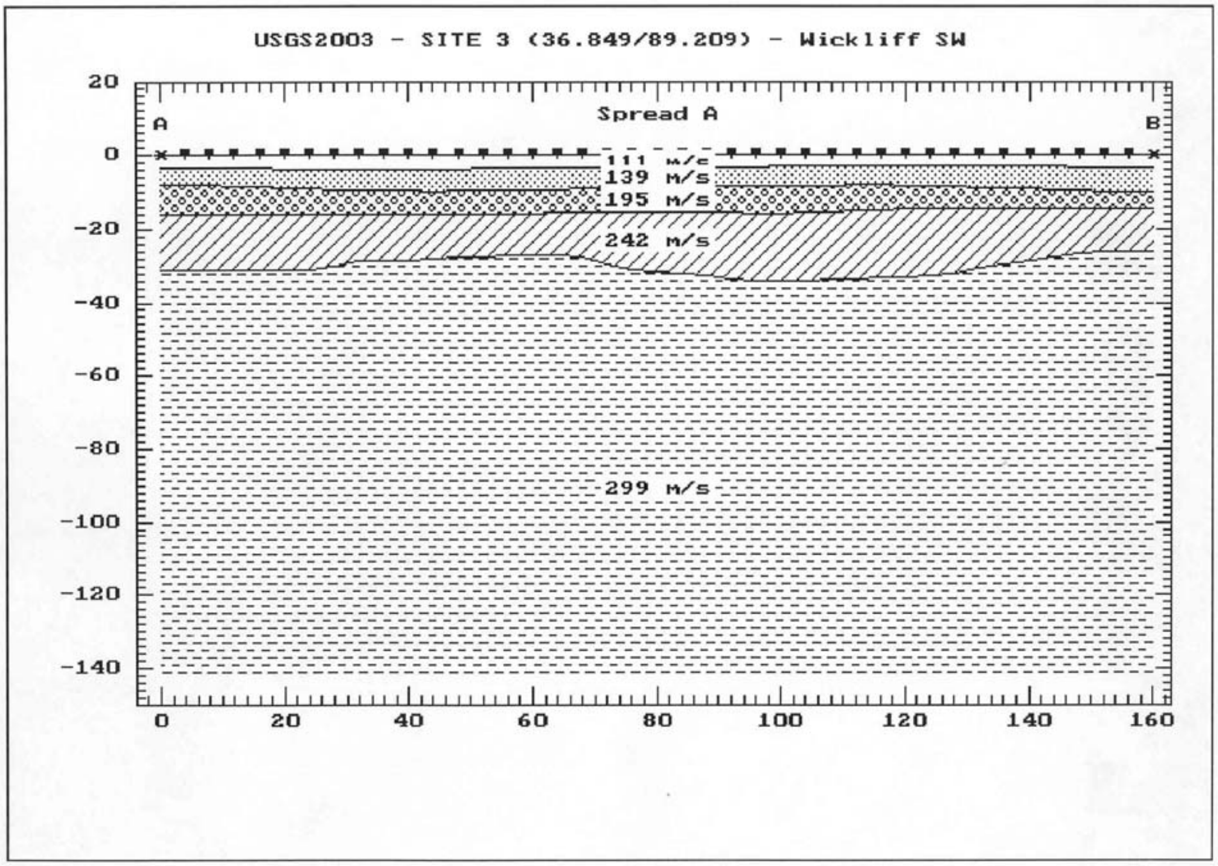

USGS2003 - SITE 3 (36.849/89.209) - Wickliff SW
Spread A
A
B
111 m/s
139 m/s
195 m/s
242 m/s
299 m/s
20
0
-20
-40
-60
-80
-100
-120
-140
0
20
40
60
80
100
120
140
160

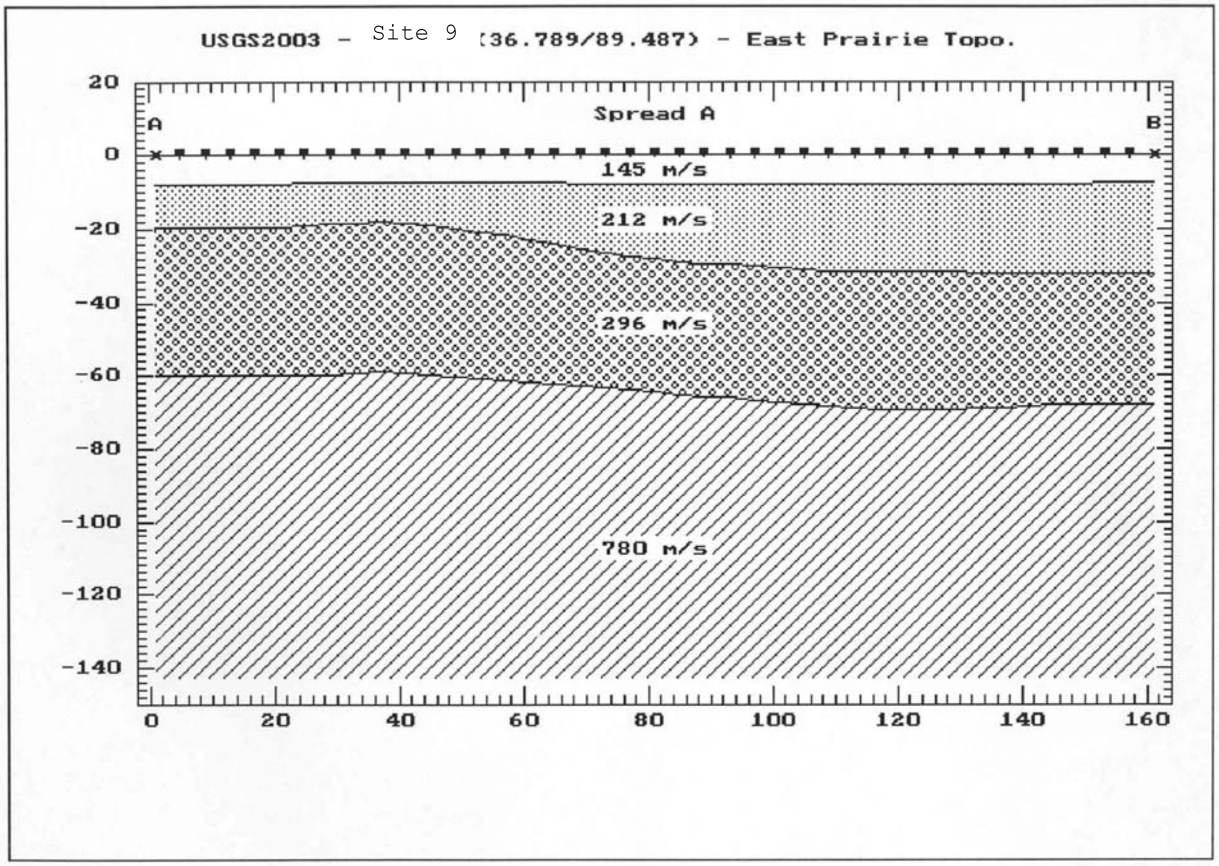
USGS2003 - Site 9 (36.789/89.487) - East Prairie Topo.
Spread A
A
B
145 m/s
212 m/s
296 m/s
780 m/s
20
0
-20
-40
-60
-80
-100
-120
-140
0
20
40
60
80
100
120
140
160

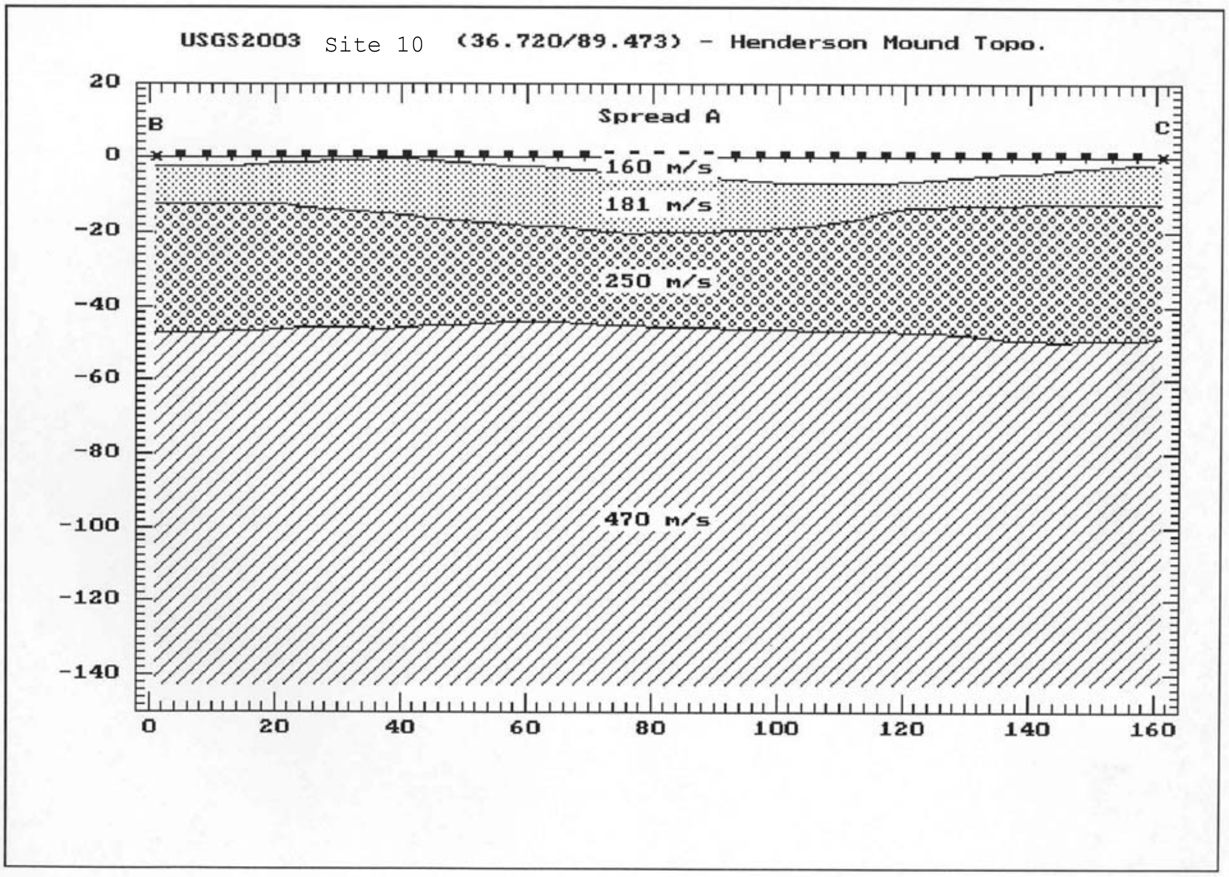
USGS2003 Site 10 (36.720/89.473) - Henderson Mound Topo.
Spread A
B
C
160 m/s
181 m/s
250 m/s
470 m/s
20
0
-20
-40
-60
-80
-100
-120
-140
0
20
40
60
80
100
120
140
160

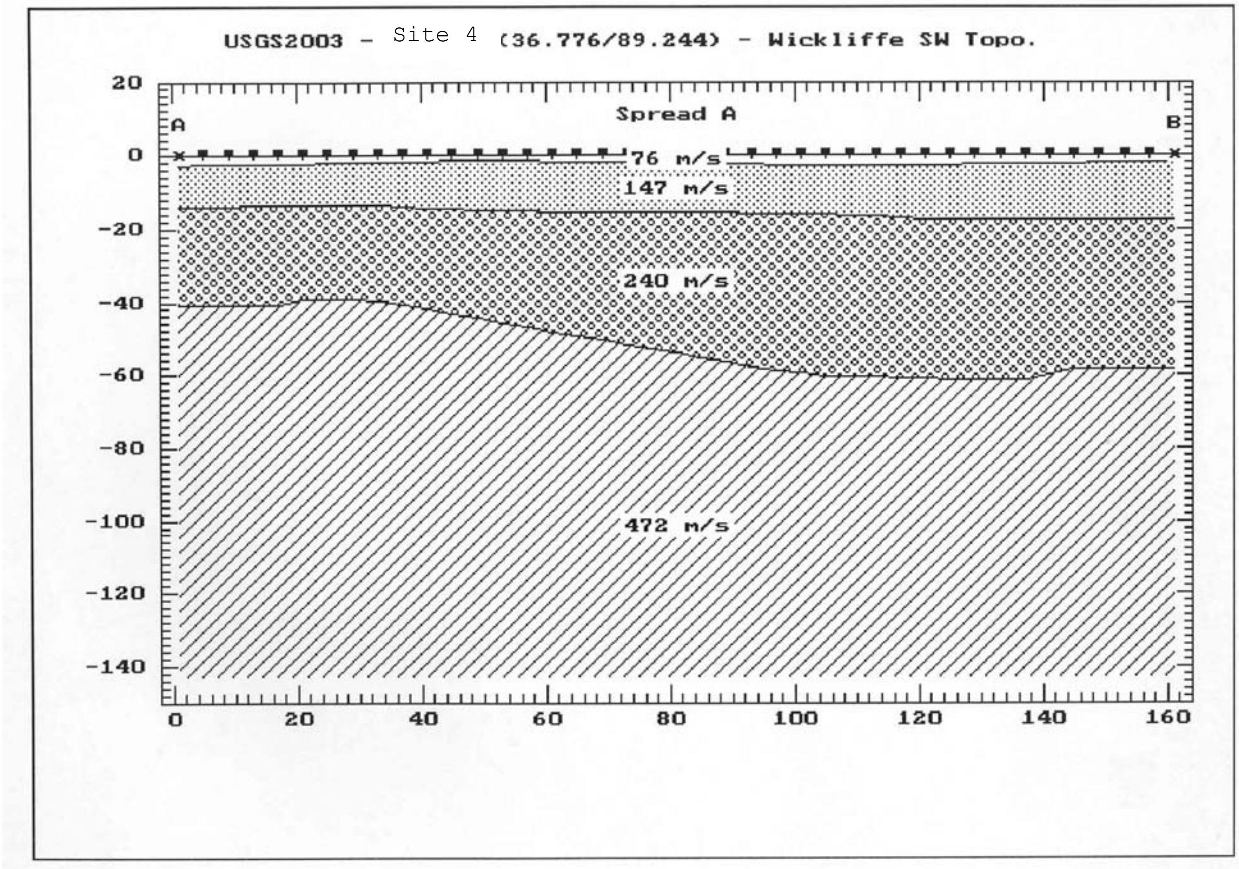

USGS2003 - Site 4 (36.776/89.244) - Wickliffe SW Topo.
Spread A
A
B
76 m/s
147 m/s
240 m/s
472 m/s
20
0
-20
-40
-60
-80
-100
-120
-140
0
20
40
60
80
100
120
140
160

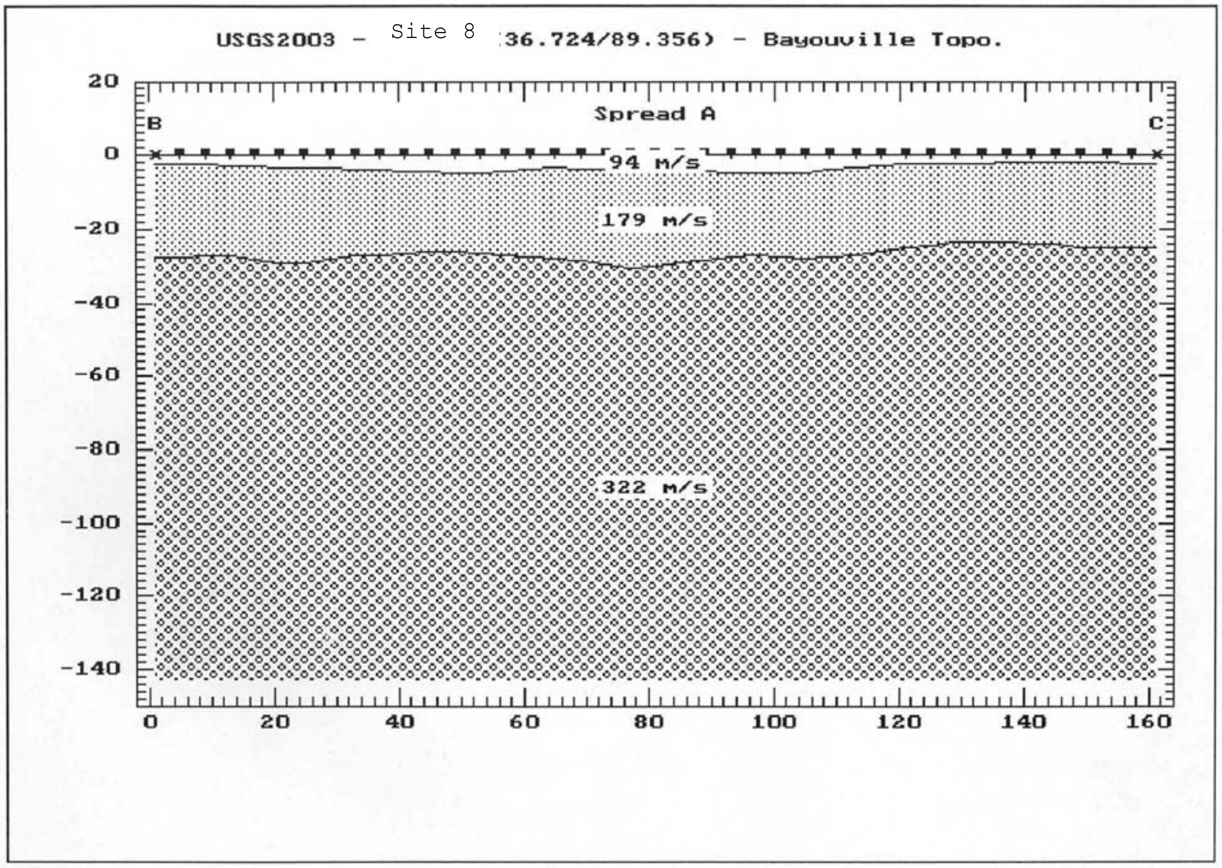
USGS2003 - Site 8 (36.724/89.356) - Bayouville Topo.
Spread A
B
C
94 m/s
179 m/s
322 m/s
20
0
-20
-40
-60
-80
-100
-120
-140
0
20
40
60
80
100
120
140
160

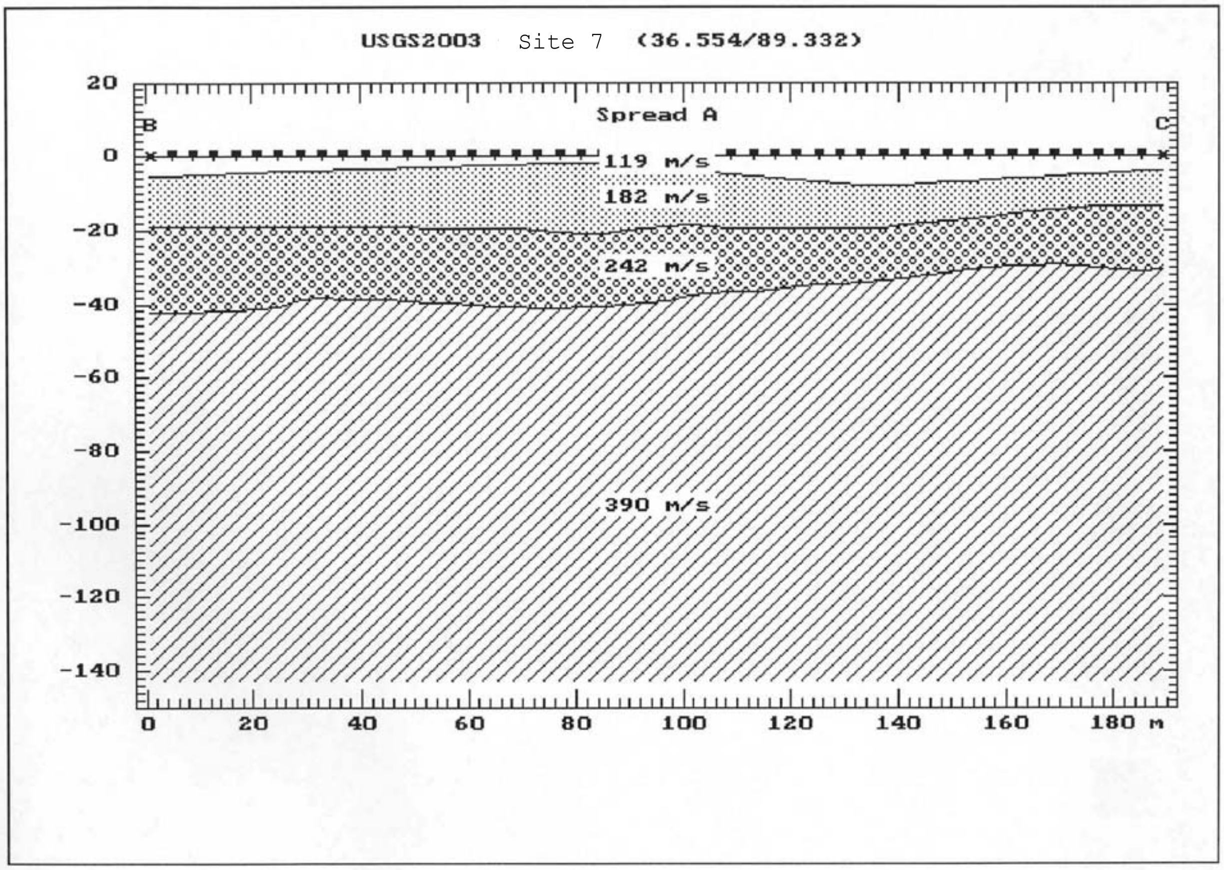
USGS2003 Site 7 (36.554/89.332)
Spread A
B
C
119 m/s
182 m/s
242 m/s
390 m/s
20
0
-20
-40
-60
-80
-100
-120
-140
0
20
40
60
80
100
120
140
160
180 m

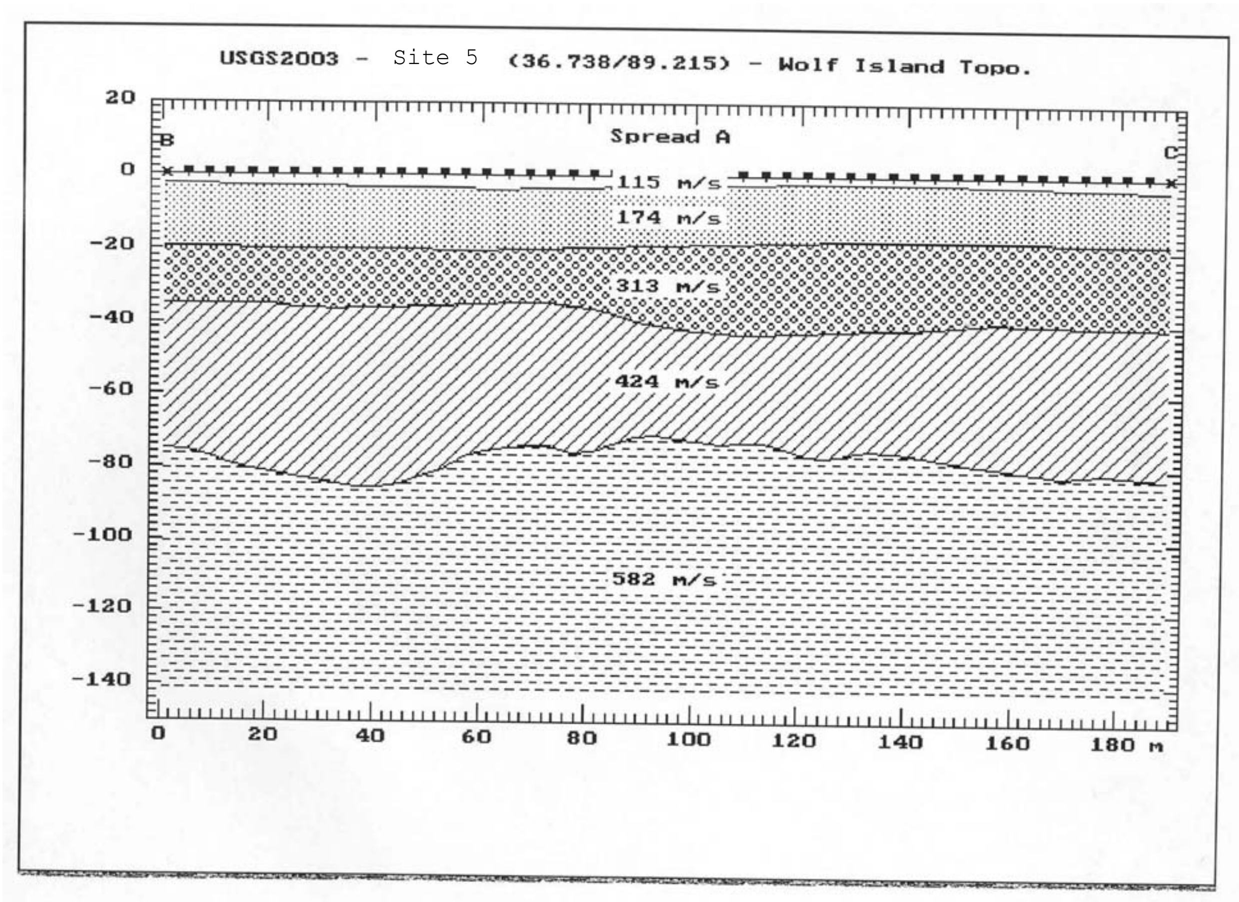
USGS2003 - Site 5 (36.738/89.215) - Wolf Island Topo.
Spread A
B
C
115 m/s
174 m/s
313 m/s
424 m/s
582 m/s
20
0
-20
-40
-60
-80
-100
-120
-140
0
20
40
60
80
100
120
140
160
180 m

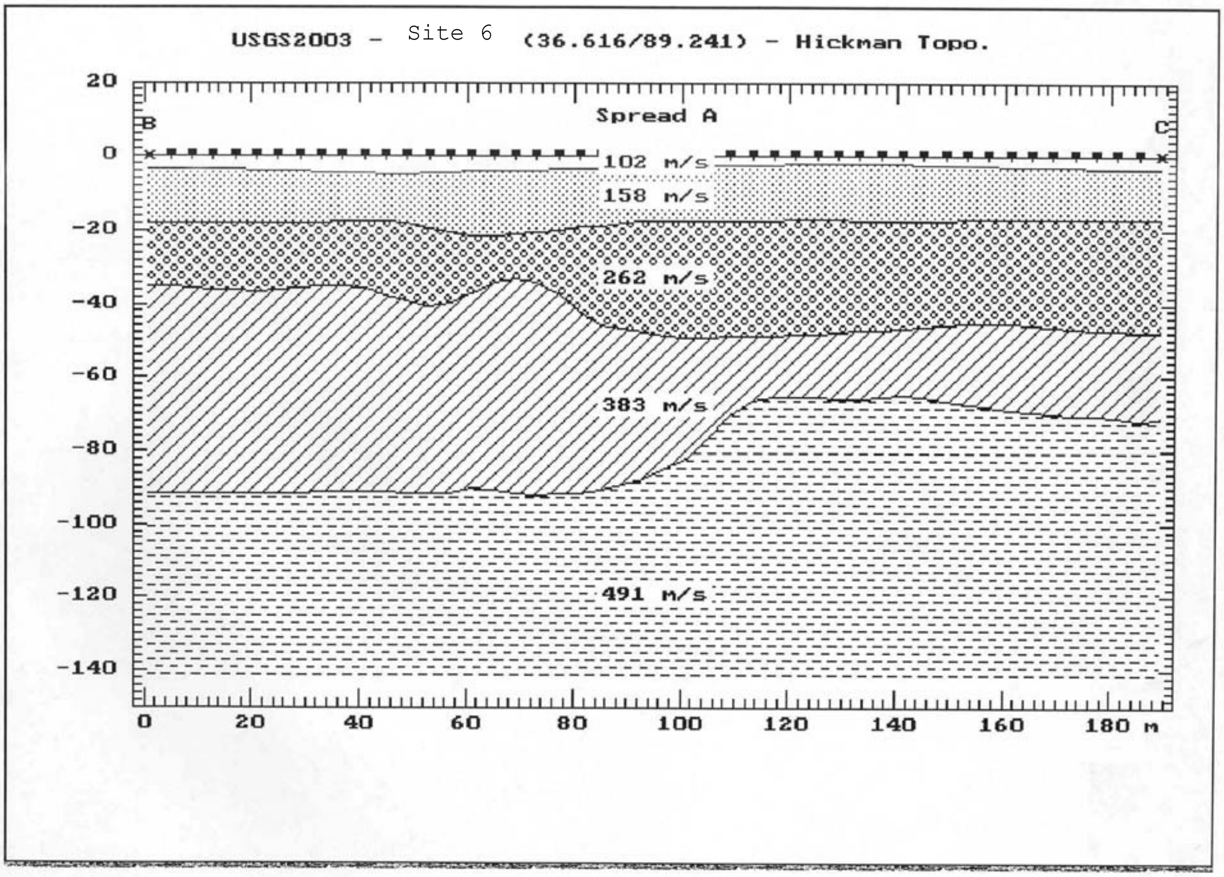

USGS2003 - Site 6 (36.616/89.241) - Hickman Topo.
Spread A
B
C
102 m/s
158 m/s
262 m/s
383 m/s
491 m/s
20
0
-20
-40
-60
-80
-100
-120
-140
0
20
40
60
80
100
120
140
160
180 m

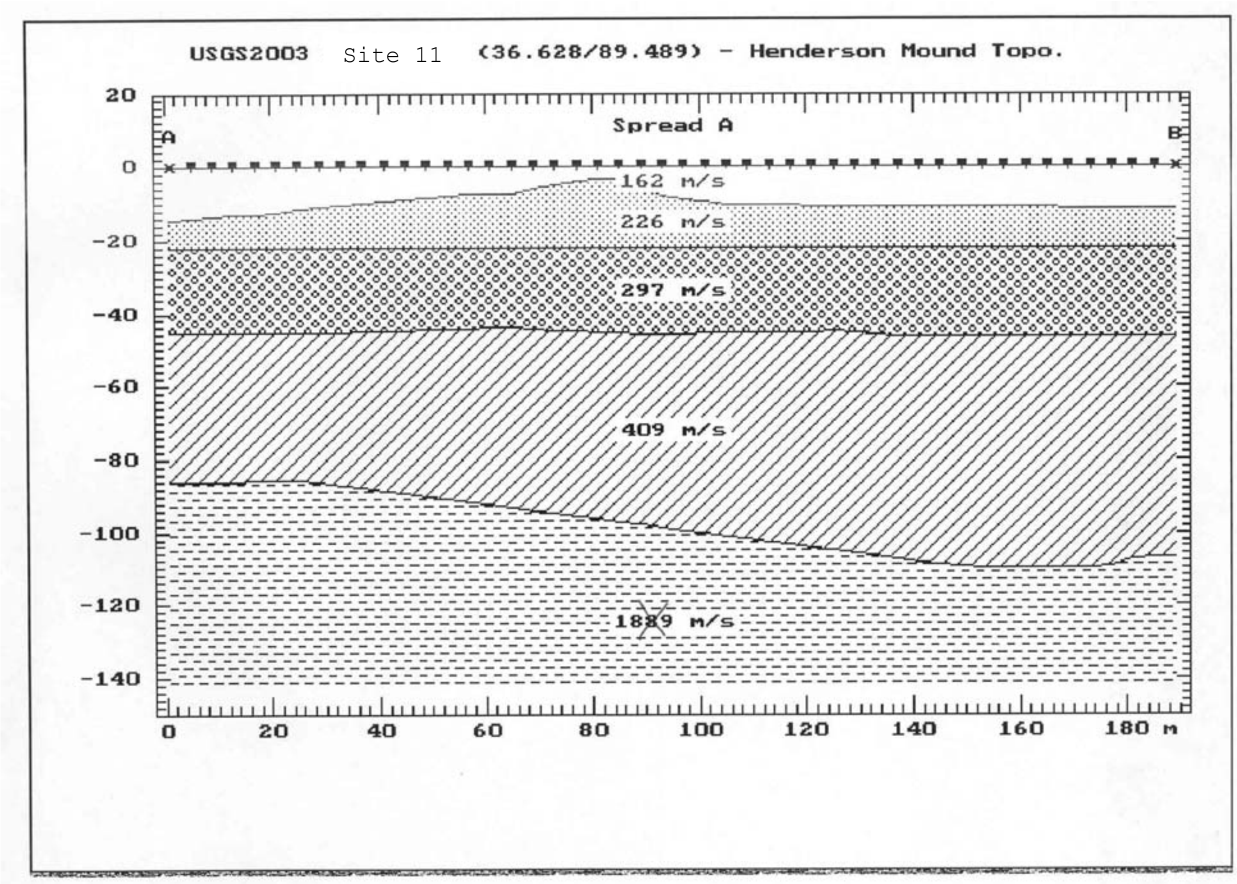
USGS2003 Site 11 (36.628/89.489) - Henderson Mound Topo.
Spread A
A
B
162 m/s
226 m/s
297 m/s
409 m/s
1889 m/s
20
0
-20
-40
-60
-80
-100
-120
-140
0
20
40
60
80
100
120
140
160
180 m

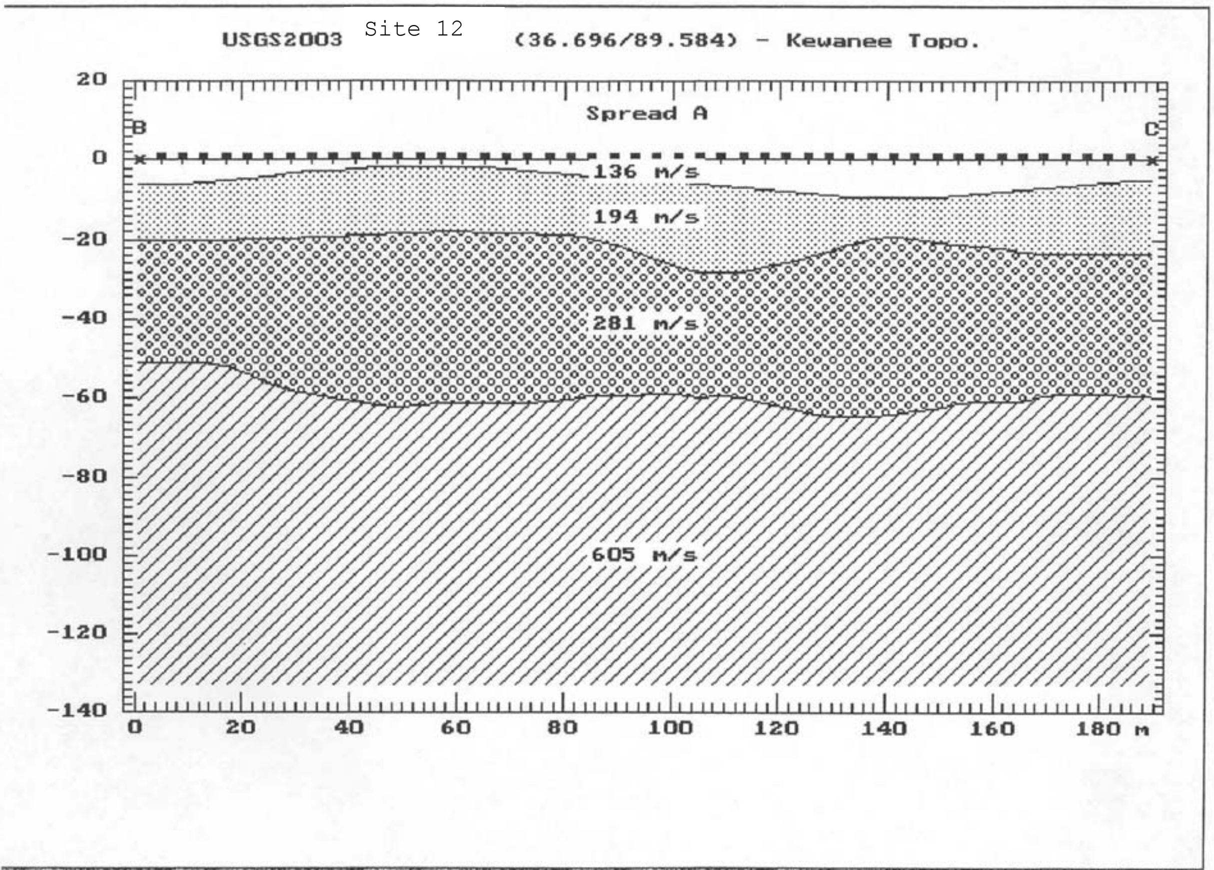

USGS2003 Site 12 (36.696/89.584) - Kewanee Topo.
Spread A
B
C
136 m/s
194 m/s
281 m/s
605 m/s
20
0
-20
-40
-60
-80
-100
-120
-140
0 20 40 60 80 100 120 140 160 180 m

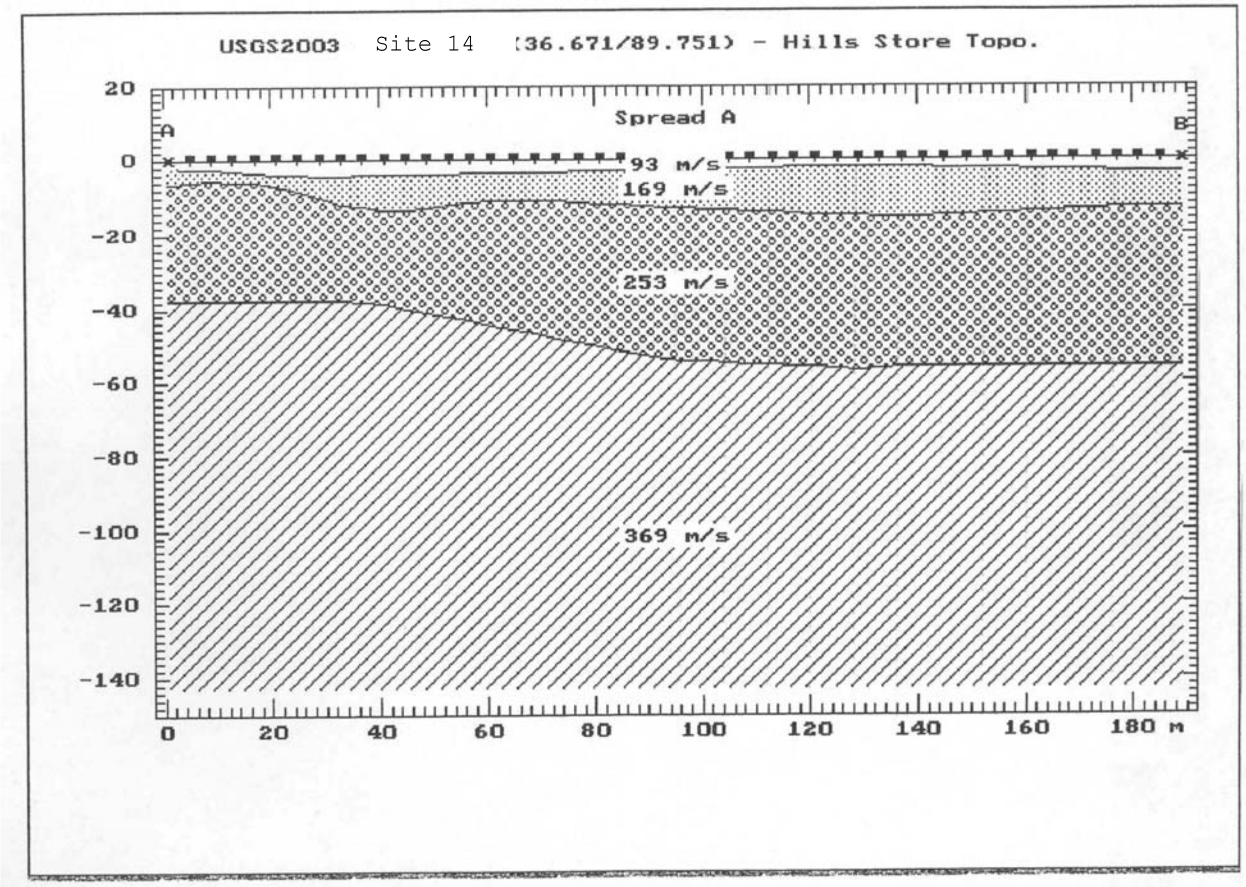
USGS2003 Site 14 (36.671/89.751) - Hills Store Topo.
Spread A
A
B
93 m/s
169 m/s
253 m/s
369 m/s
20
0
-20
-40
-60
-80
-100
-120
-140
0
20
40
60
80
100
120
140
160
180 m

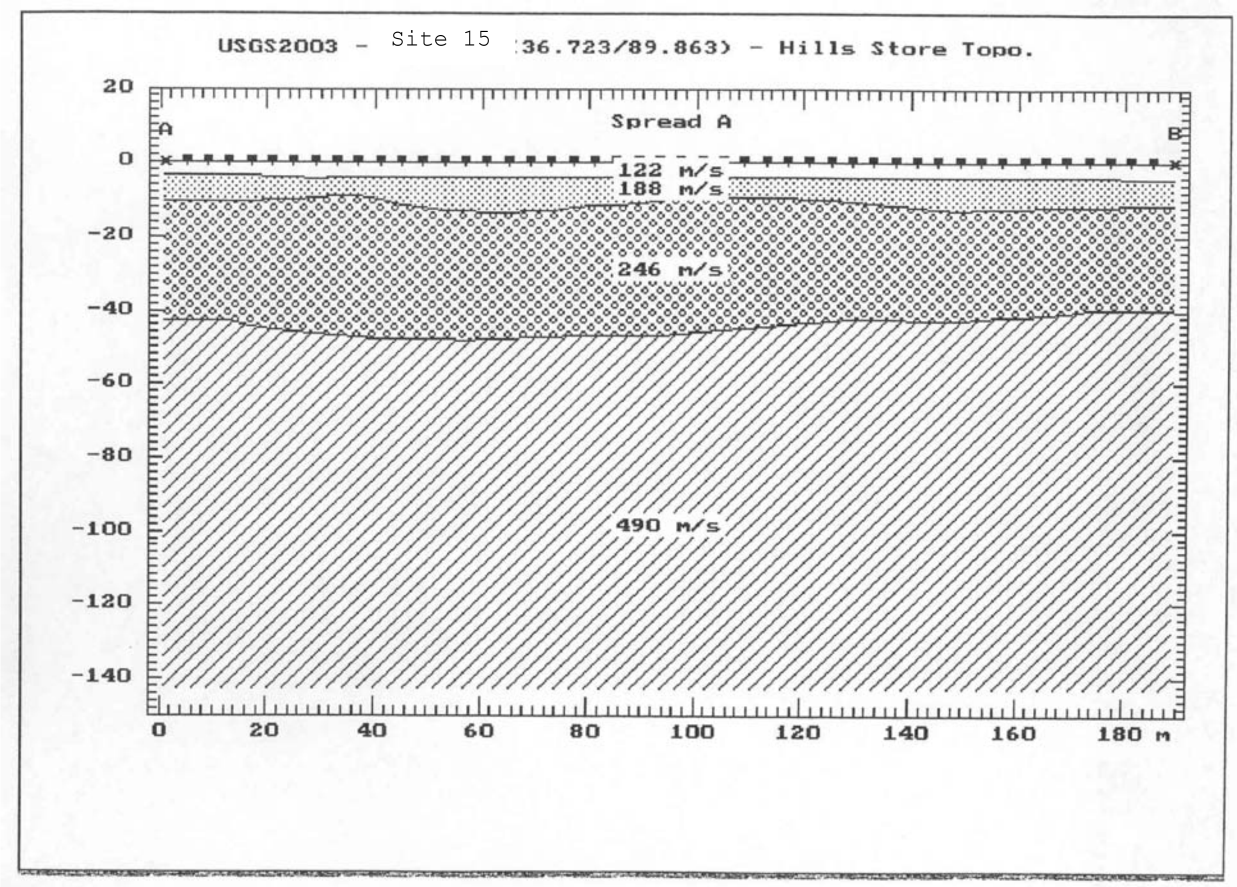

USGS2003 - Site 15 (36.723/89.863) - Hills Store Topo.
Spread A
A
B
122 m/s
188 m/s
246 m/s
490 m/s
20
0
-20
-40
-60
-80
-100
-120
-140
0
20
40
60
80
100
120
140
160
180 m

APPENDIX B

SITE VELOCITY MODELS

Site: 1

Location: 36.971°N/89.207°W
Elevation: 96 m

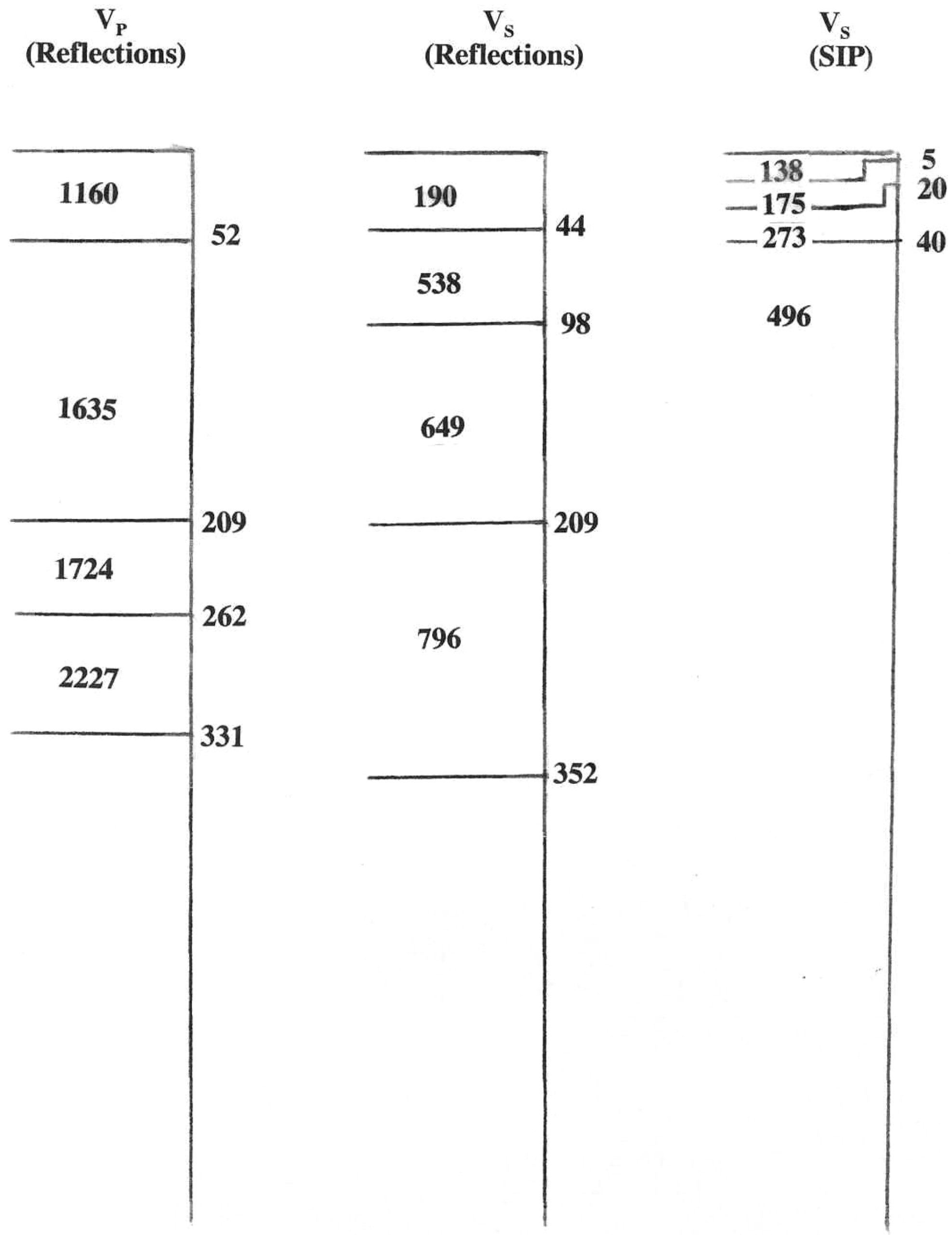

* Velocities are in m/s, and depths are in m.

Site: 2

Location: 36.892°N/89.222°W
Elevation: 94 m

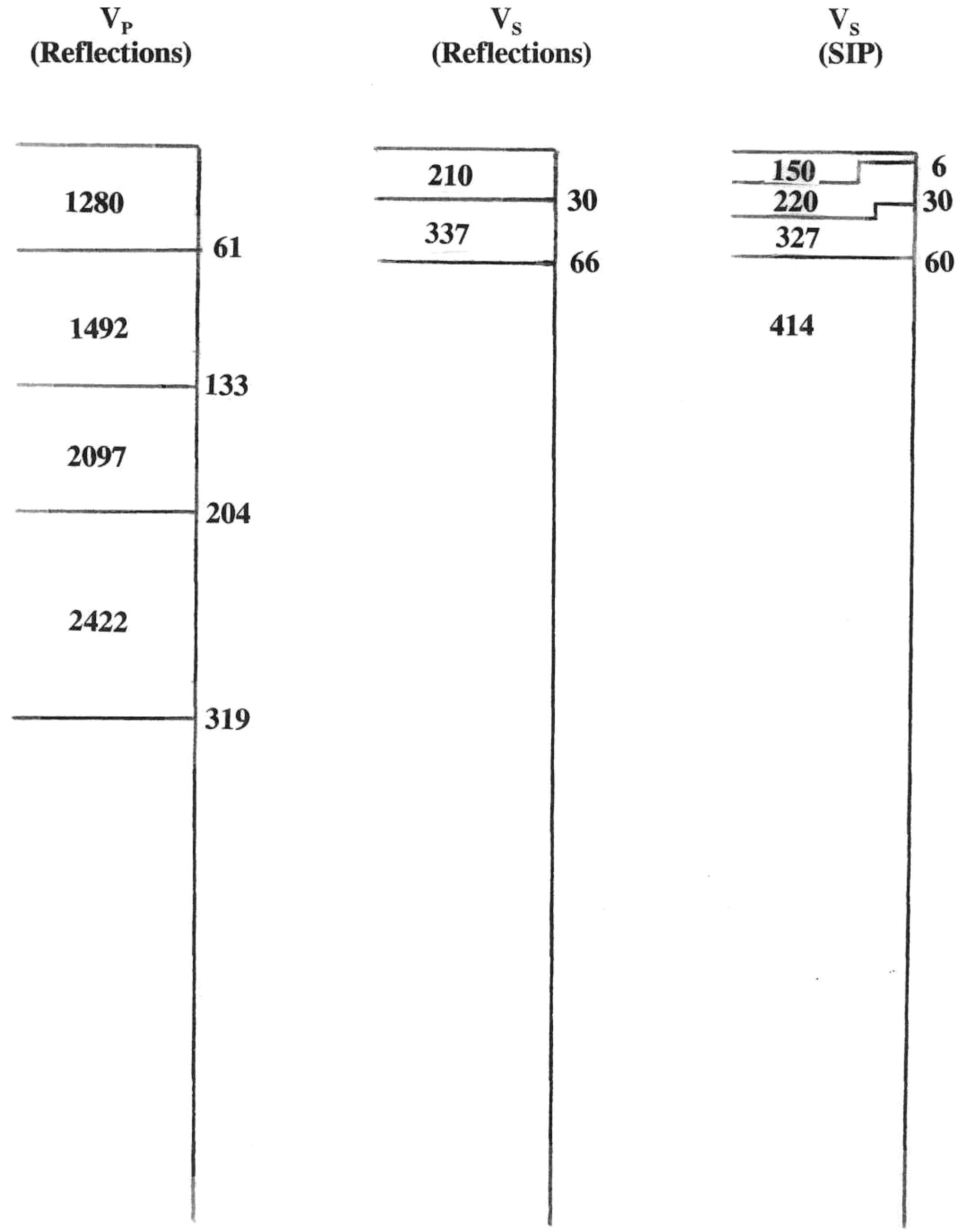

* Velocities are in m/s, and depths are in m.

<u>Site</u>: **3**

Location: **36.849°N/89.209°W**
Elevation: **93 m**

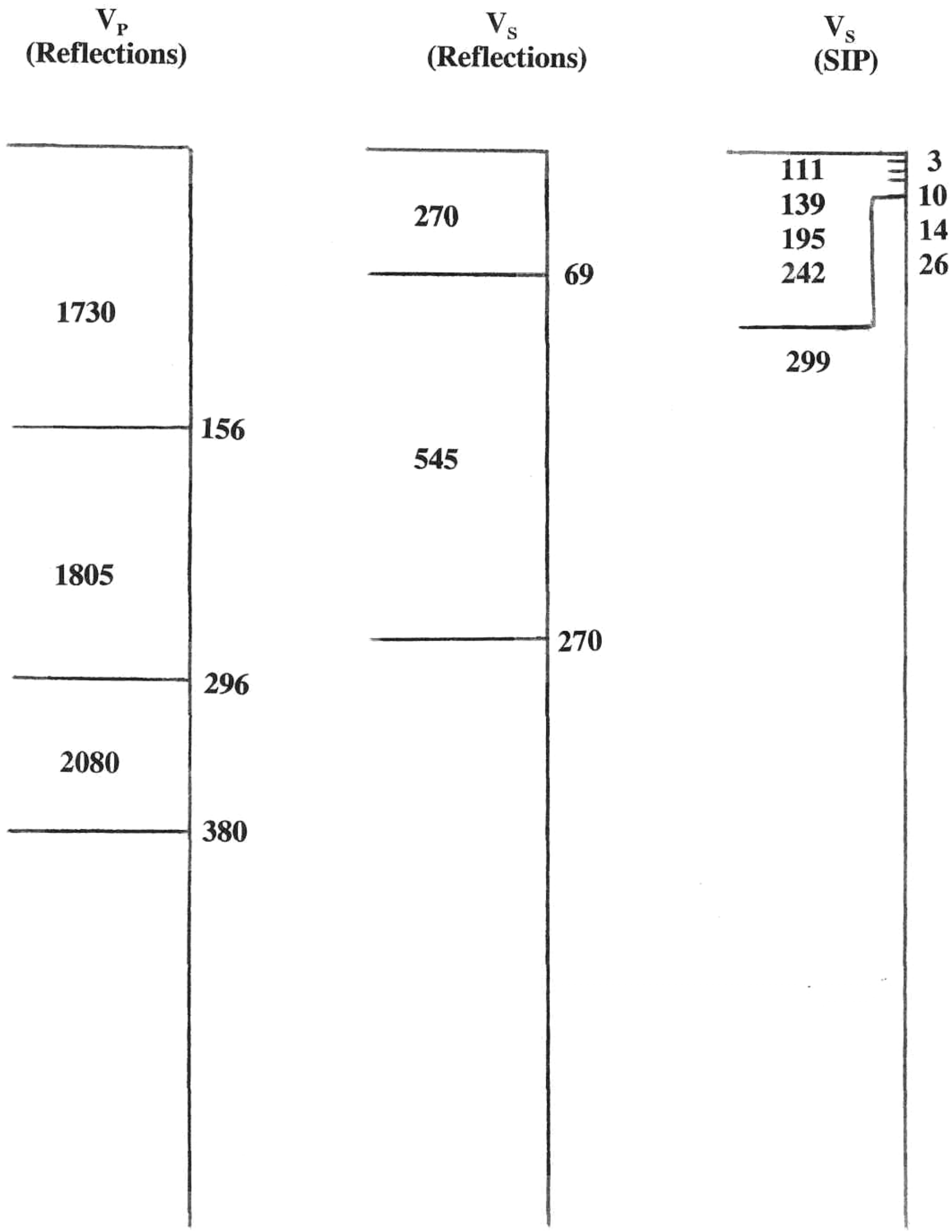

*** Velocities are in m/s, and depths are in m.**

Site: 4

Location: 36.776°N/89.244°W
Elevation: 91 m

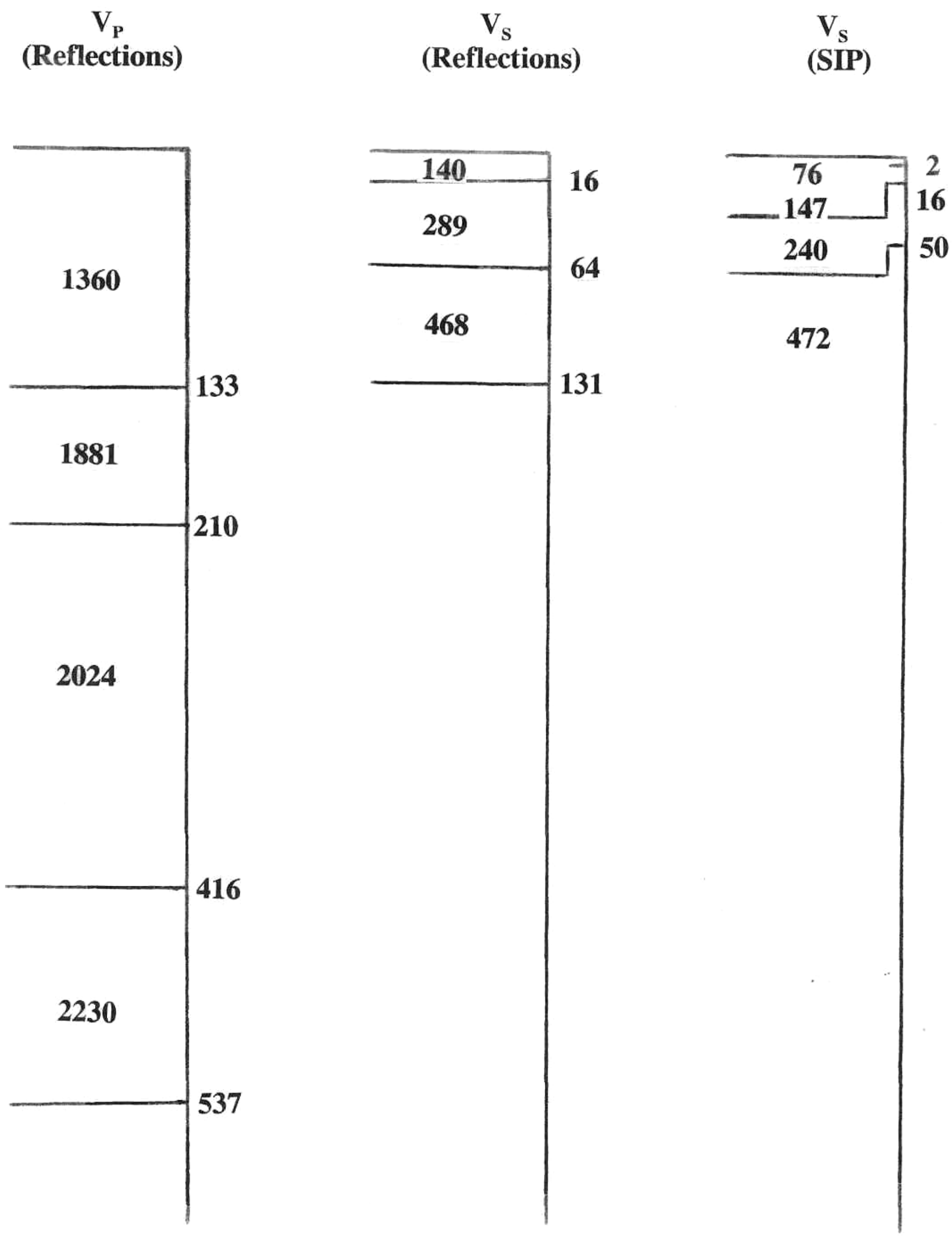

* Velocities are in m/s, and depths are in m.

Site: 5

Location: 36.738°N/89.215°W
Elevation: 92 m

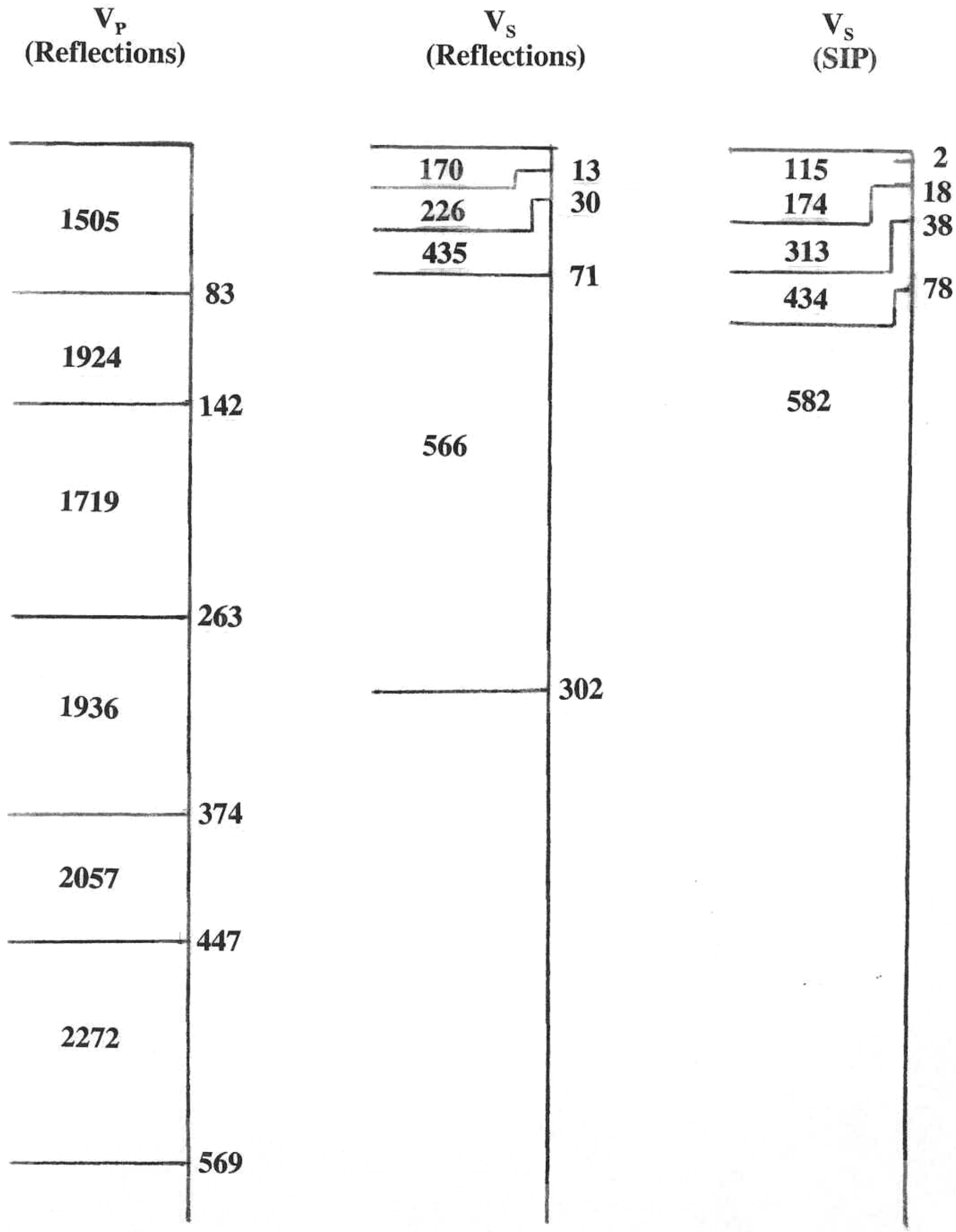

* Velocities are in m/s, and depths are in m.

Site: 6

Location: 36.616°N/89.241°W
Elevation: 91 m

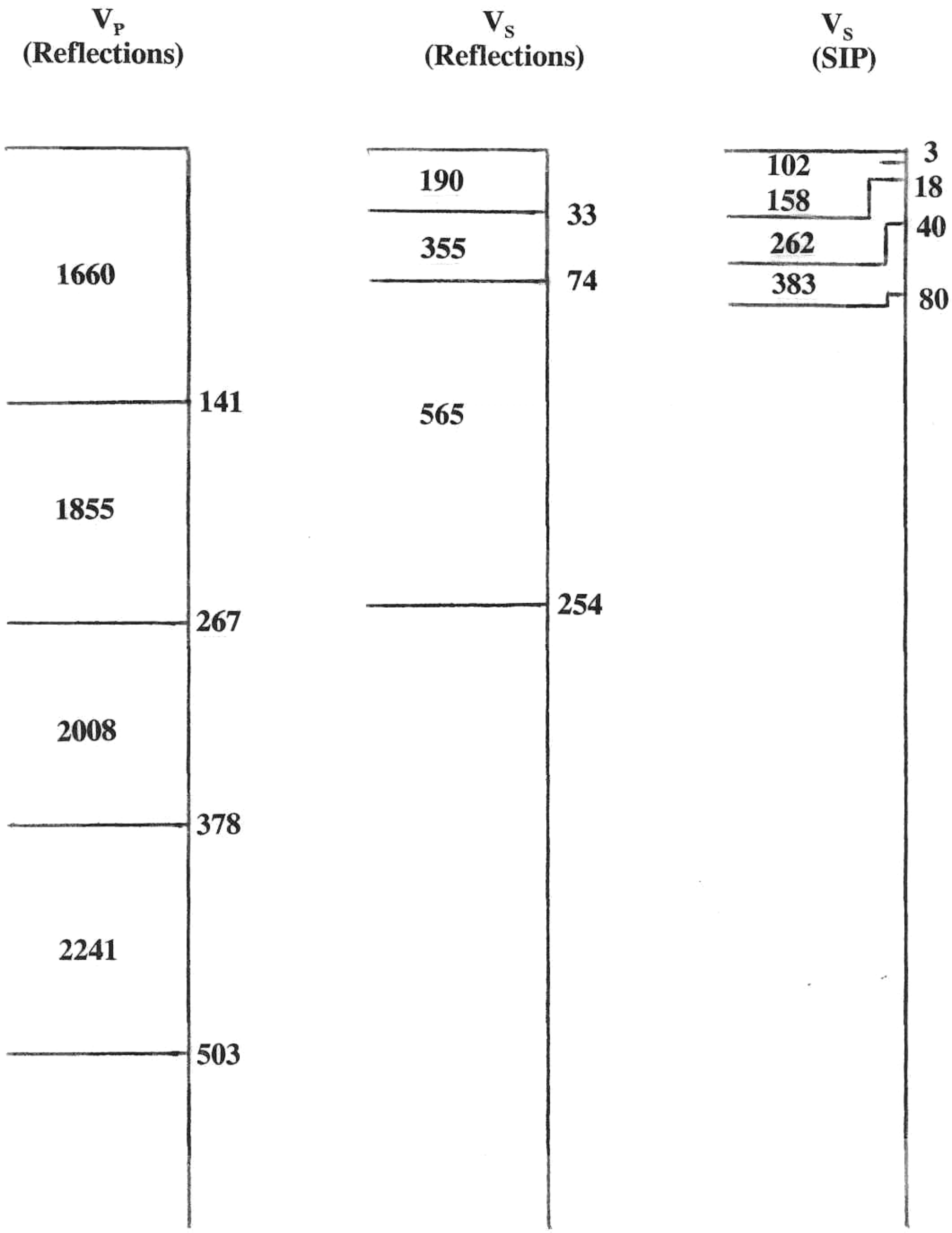

* Velocities are in m/s, and depths are in m.

Site: 7

Location: 36.554°N/89.332°W
Elevation: 100 m

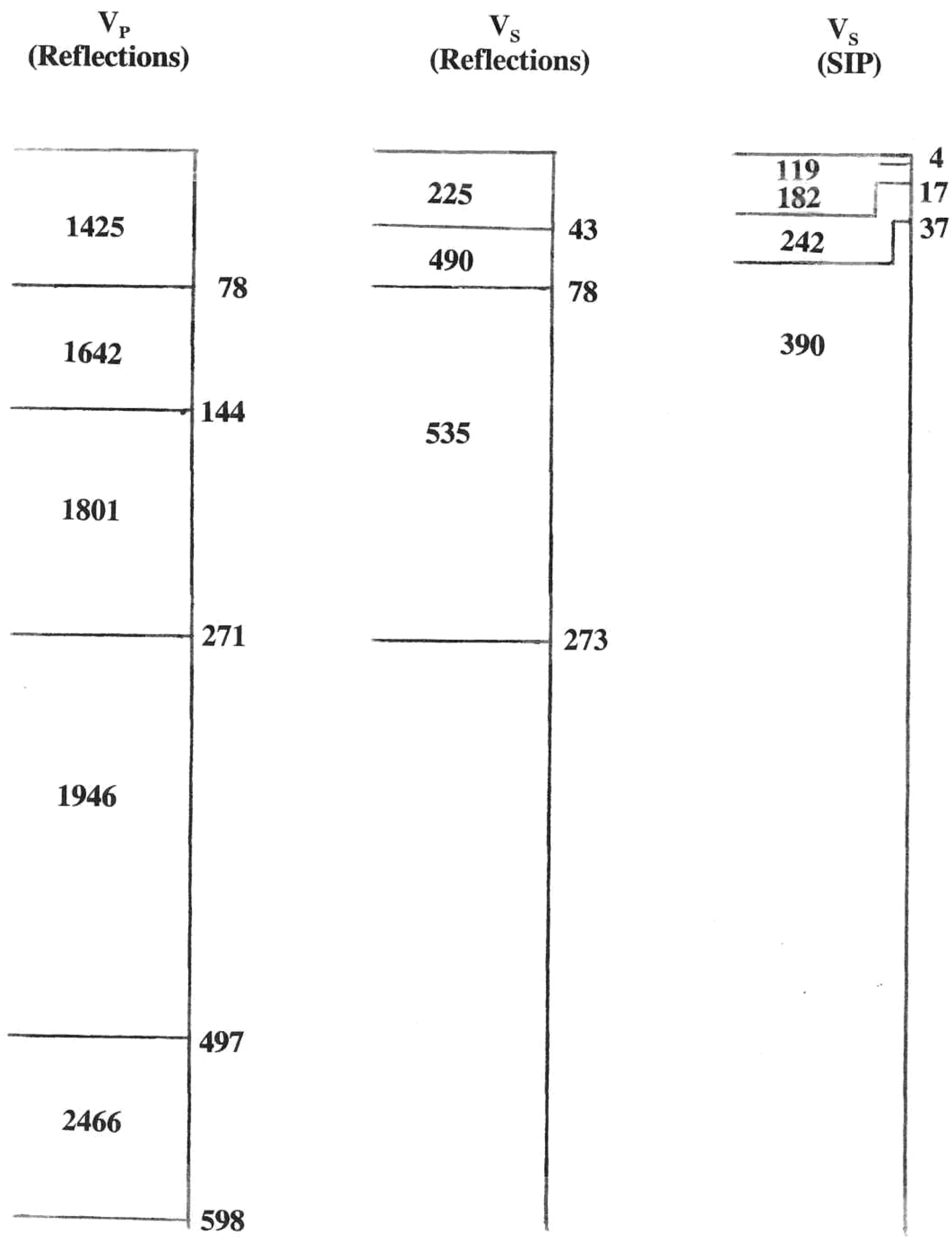

* Velocities are in m/s, and depths are in m.

Site: 8 (near EPRM)

Location: 36.724°N/89.356°W
Elevation: 90 m

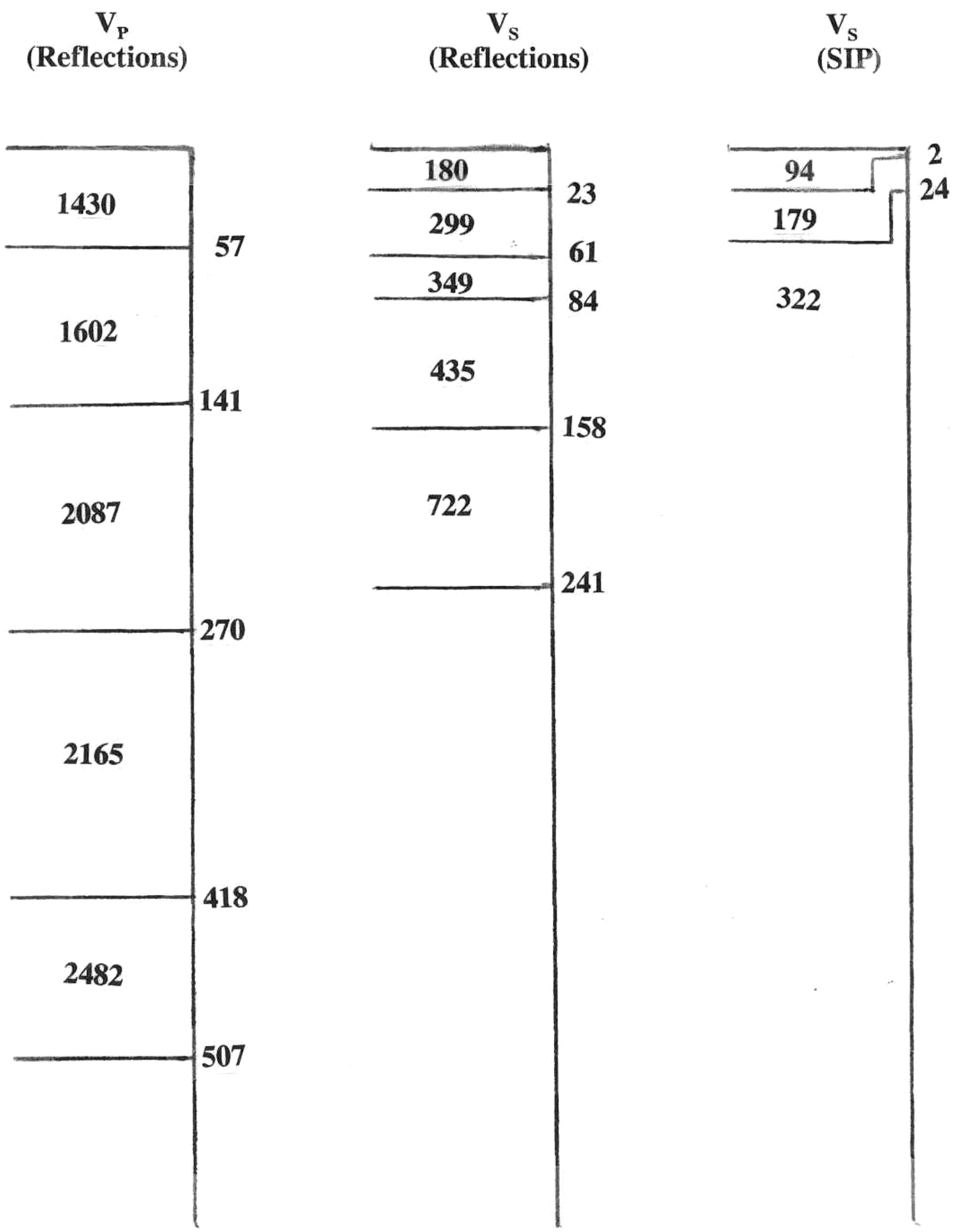

*** Velocities are in m/s, and depths are in m.**

Site: 9 (near DWDM)

Location: 36.789°N/89.487°W
Elevation: 91 m

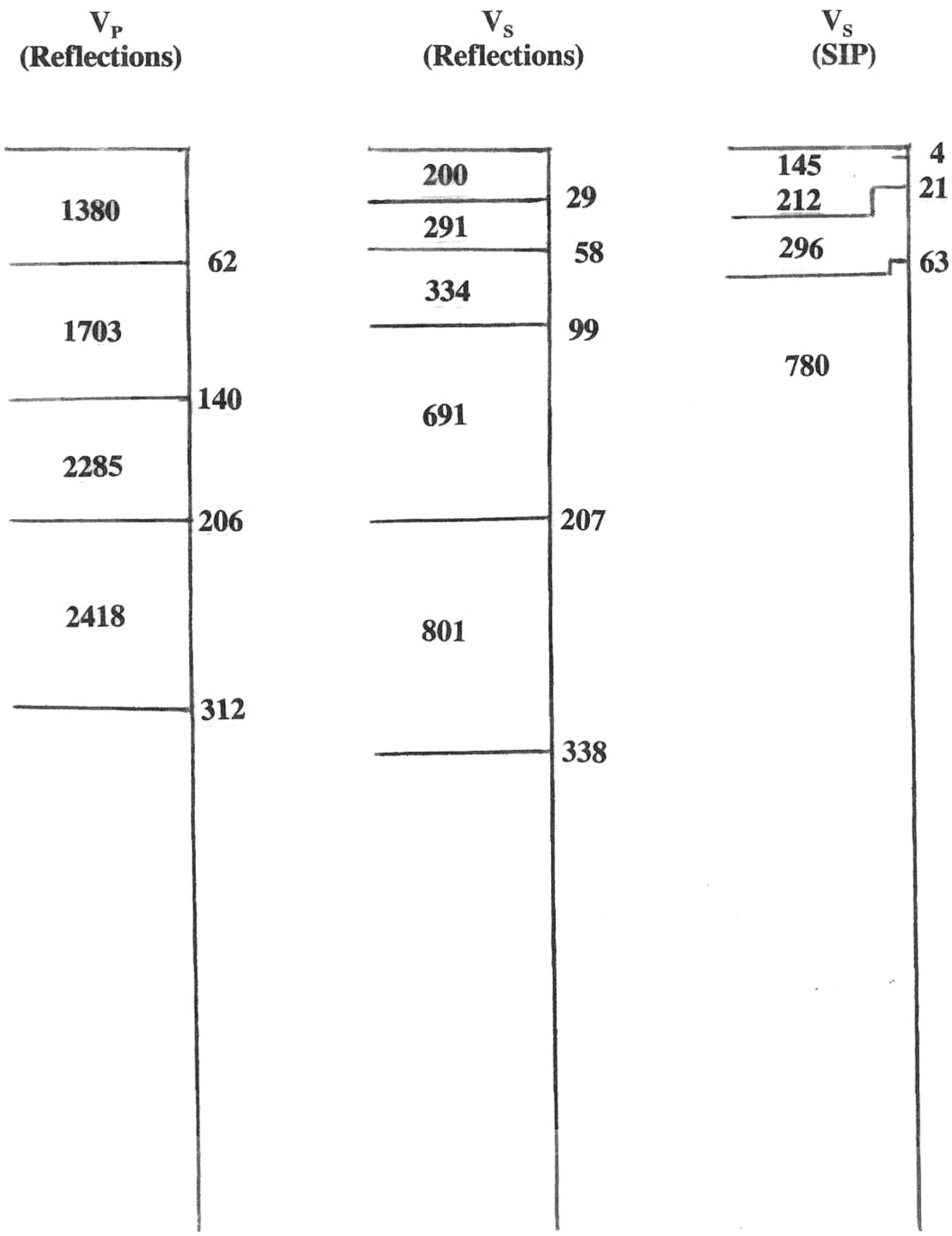

*** Velocities are in m/s, and depths are in m.**

Site: 10 (near HENM)

Location: 36.720°N/89.473°W
Elevation: 90 m

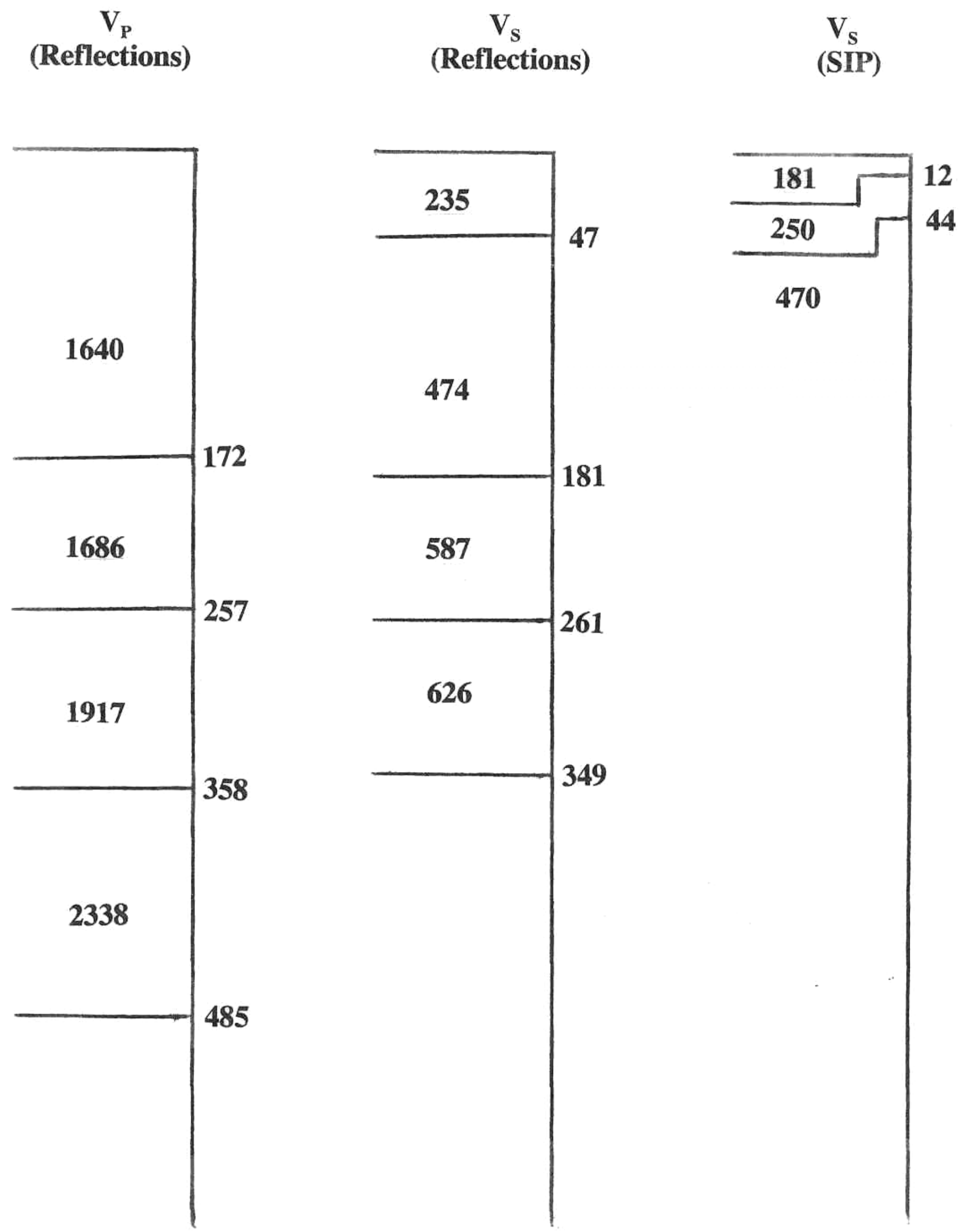

* Velocities are in m/s, and depths are in m.

Site: 11 (near SJBM)

Location: 36.628°N/89.489°W
Elevation: 91 m

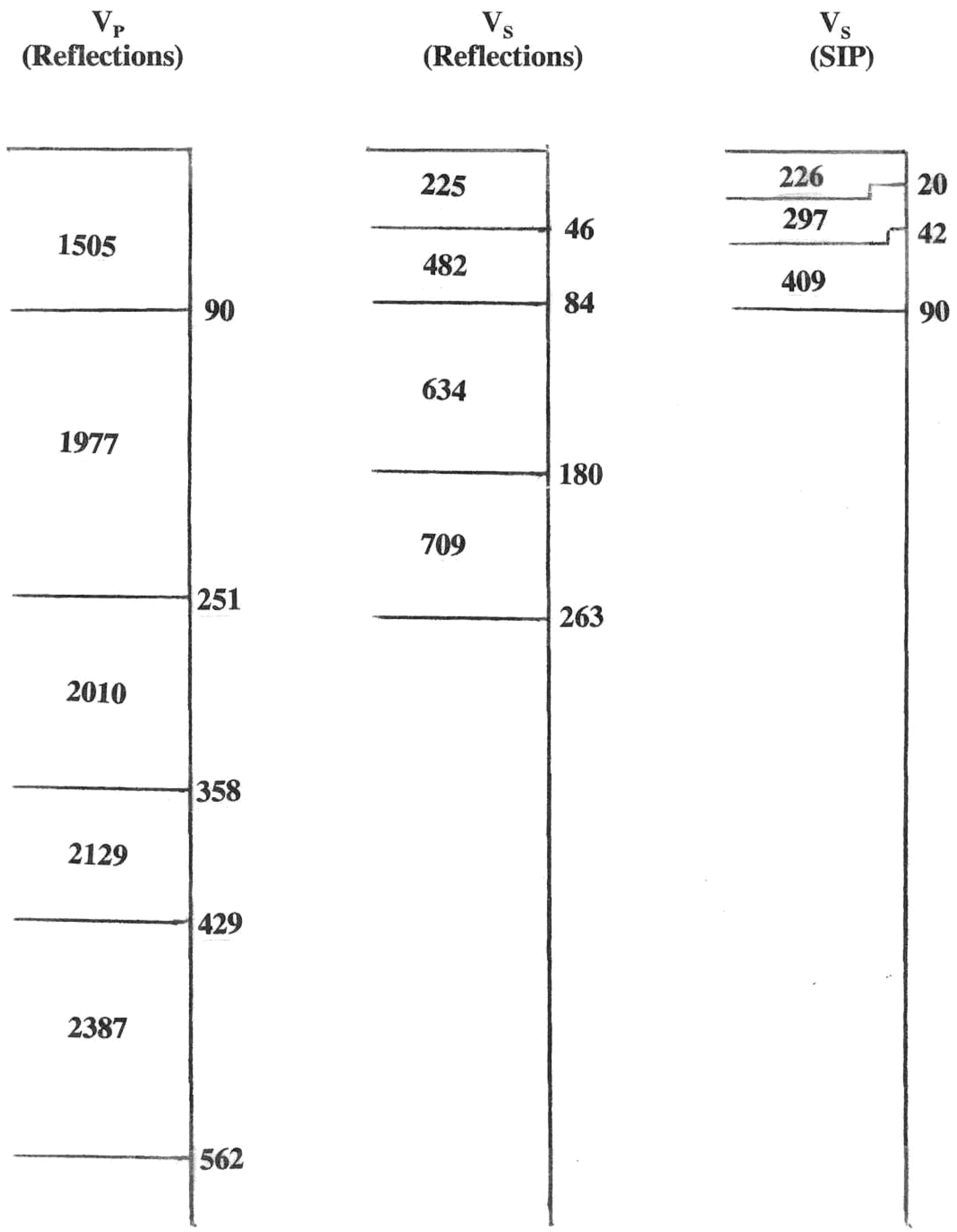

* Velocities are in m/s, and depths are in m.

Site: 12 (near KEWM)

Location: 36.696°N/89.584°W
Elevation: 88 m

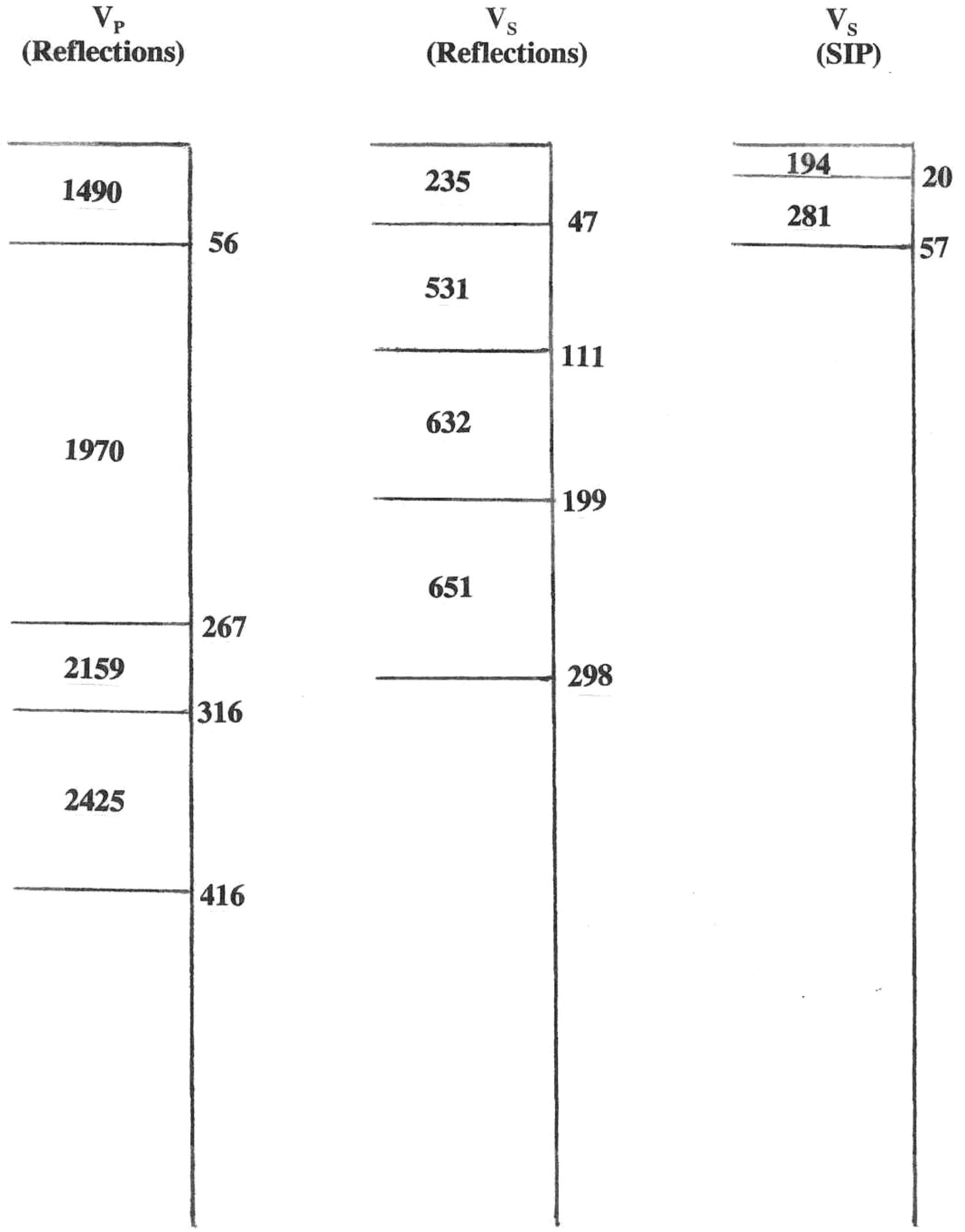

*** Velocities are in m/s, and depths are in m.**

Site: 13 (near COKM)

Location: 36.715°N/89.734°W
Elevation: 87 m

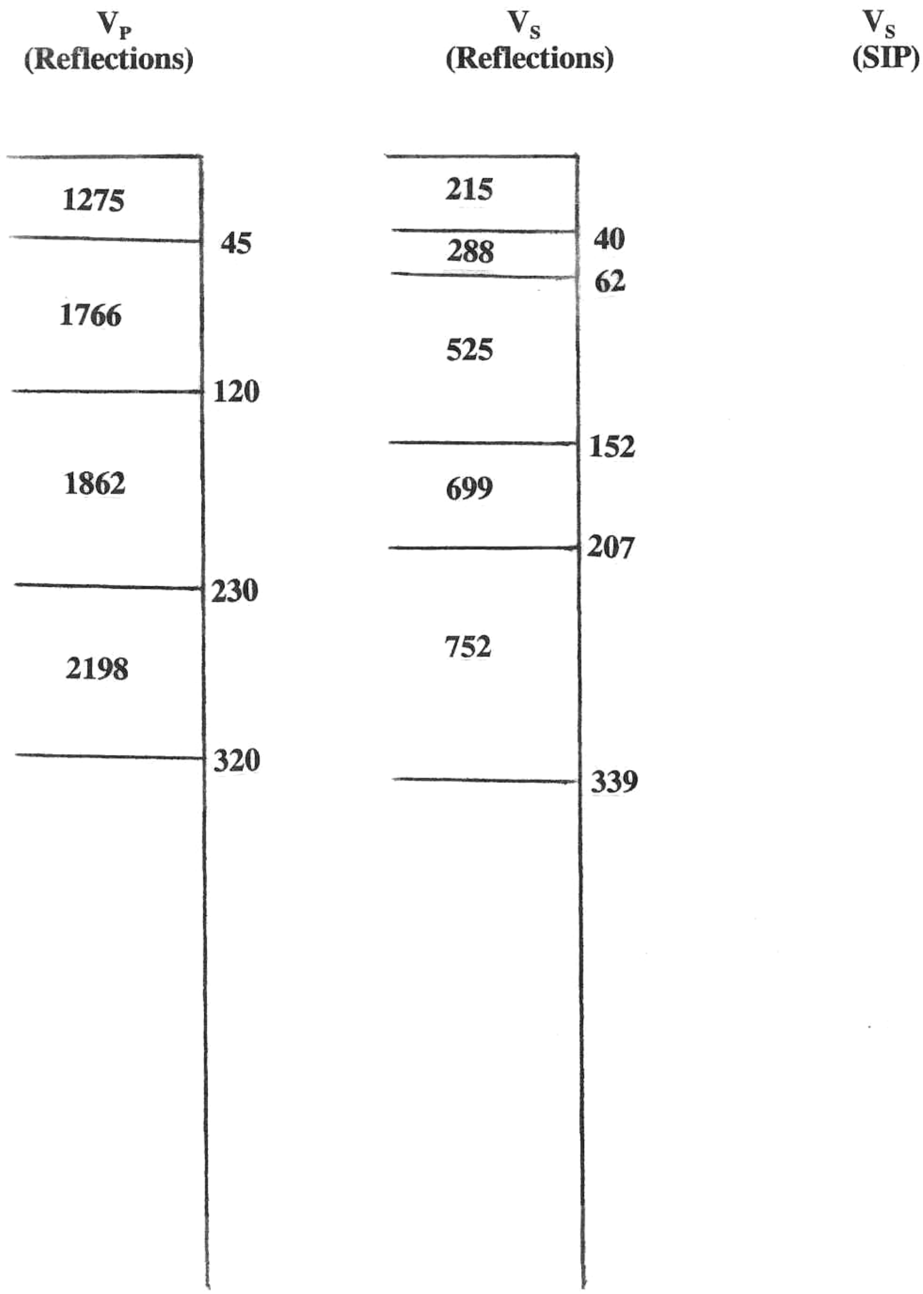

* Velocities are in m/s, and depths are in m.

Site: 14 (near PARM)

Location: 36.671°N/89.751°W
Elevation: 87 m

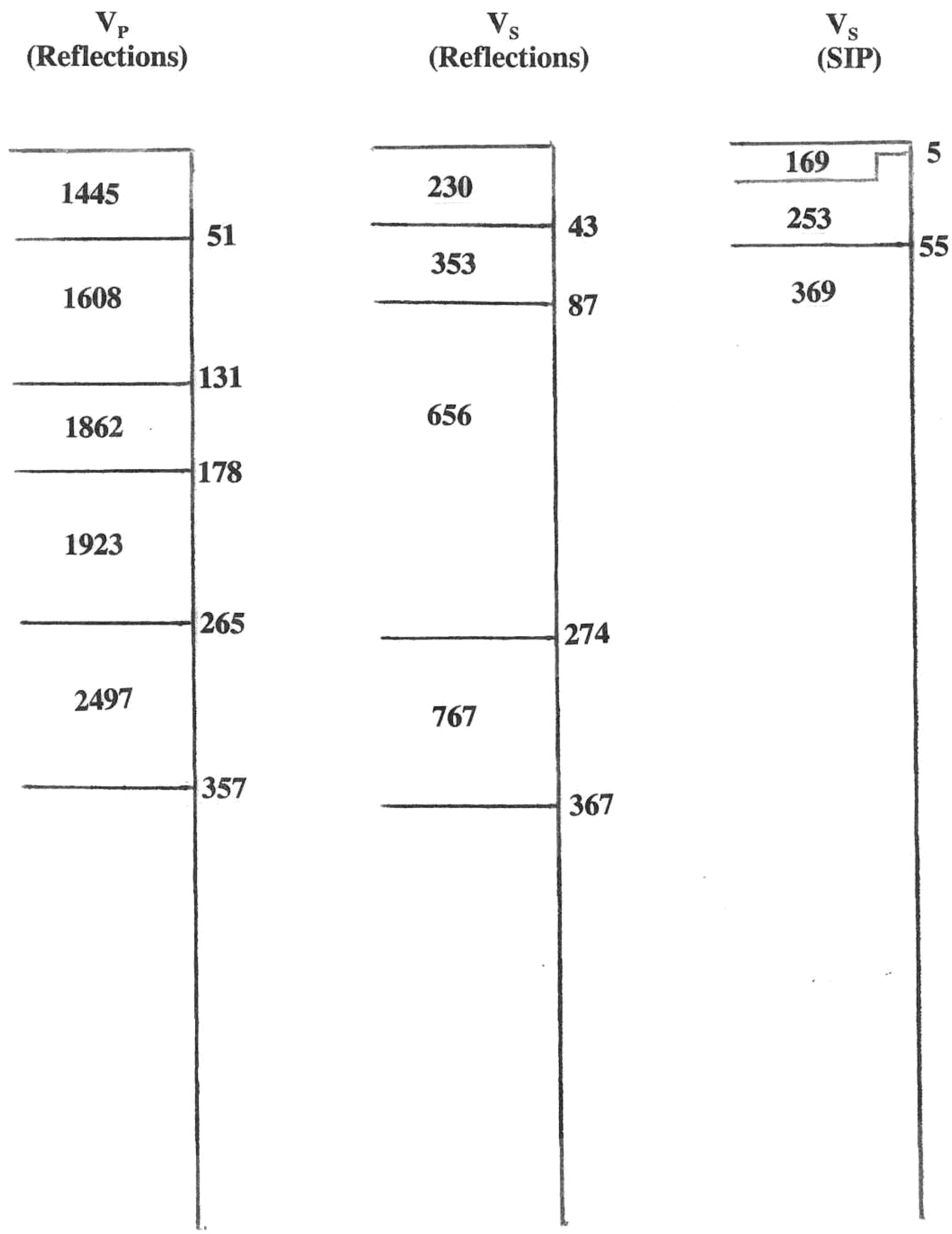

* Velocities are in m/s, and depths are in m.

Site: 15 (near BACM)

Location: 36.723°N/89.863°W
Elevation: 87 m

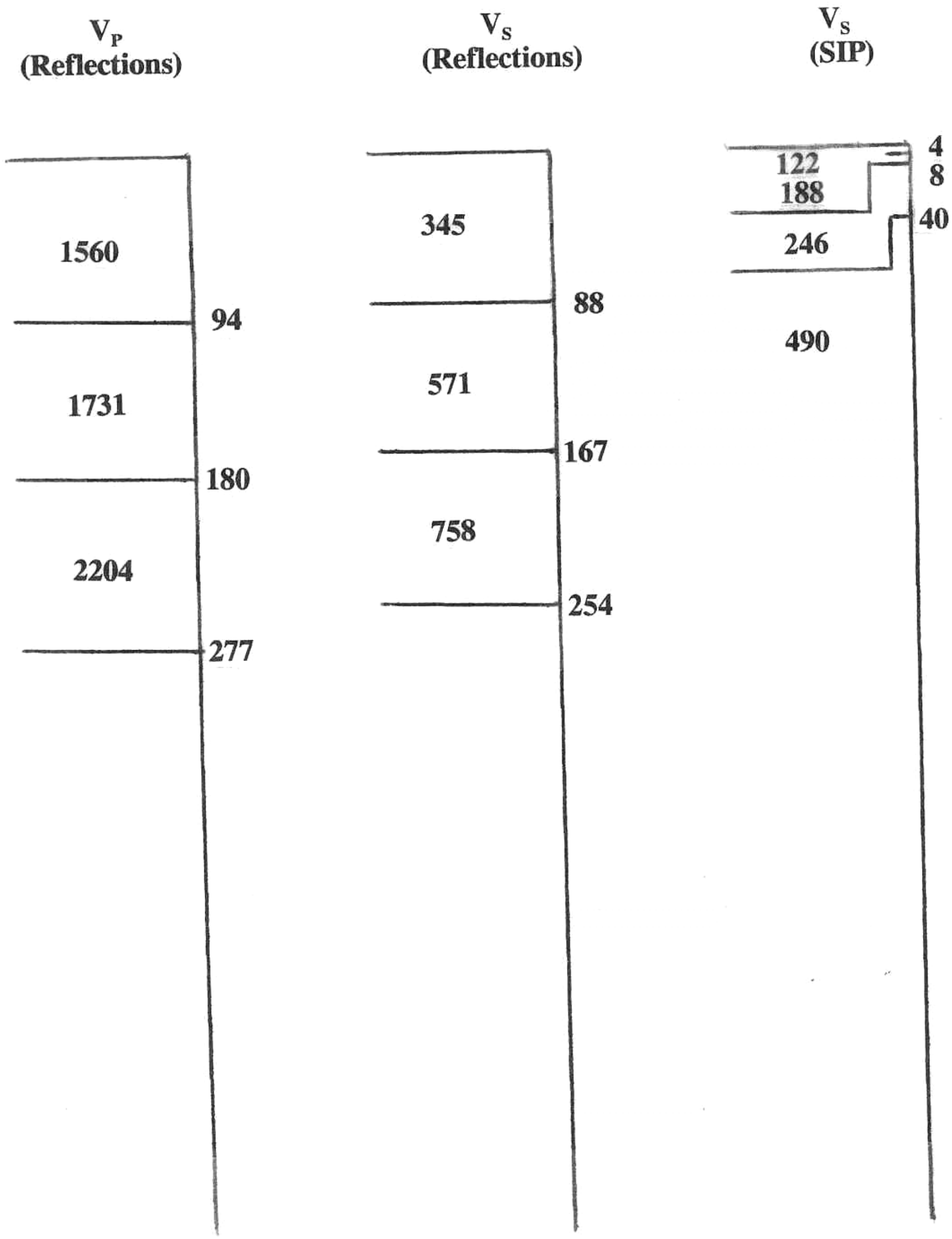

* Velocities are in m/s, and depths are in m.